

# Sensitivity of asymmetric Oxygen Minimum Zones to ~~remineralization rate and~~ mixing intensity and stoichiometry in the tropical Pacific using a basin-scale model (OGCM-DMEC V1.24)

Kai Wang<sup>1</sup>, Xiujun Wang<sup>1,2\*</sup>, Raghu Murtugudde<sup>2</sup>, Dongxiao Zhang<sup>3</sup>, Rong-Hua Zhang<sup>4</sup>

5 <sup>1</sup>College of Global Change and Earth System Science, Beijing Normal University, Beijing 100875, China

<sup>2</sup>Earth System Science Interdisciplinary Center, University of Maryland, College Park, Maryland 20740, USA

<sup>3</sup>JISAO, University of Washington and NOAA, Pacific Marine Environmental Laboratory, Seattle, Washington 98115, USA

<sup>4</sup>Institute of Oceanology, Chinese Academy of Sciences, Qingdao, Shandong 266071, China

Correspondence to: Xiujun Wang (xwang@bnu.edu.cn)

10 **Abstract.** The tropical Pacific Ocean holds the world's two largest Oxygen Minimum Zones (OMZs), showing a prominent hemispheric asymmetry, with a much stronger and broader OMZ north of the equator. However, many models have difficulties in reproducing the observed asymmetric OMZs in the tropical Pacific. Here, we apply a fully coupled basin-scale model (~~OGCM-DMEC V1.2~~) to evaluate the impacts of ~~remineralization rate~~ stoichiometry and the intensity of vertical mixing on the dynamics of OMZs in the tropical Pacific. We first utilize observational data of dissolved oxygen (DO), ~~dissolved organic~~  
15 ~~nitrogen (DON) and oxygen consumption~~ to calibrate and validate the basin-scale model. Our model experiments demonstrate that enhanced vertical mixing combined with reduced ~~remineralization rate~~ O:C utilization ratio can significantly improve our model capability of reproducing the asymmetric OMZs. Our study shows that DO is more sensitive to biological processes over 200-~~400~~700 m but to physical processes over 400-1000 m. Enhanced vertical mixing ~~not only~~ causes ~~an~~ a large increase in ~~DO~~ physical supply at mid-depth, but also results and a small increase in ~~lower rates of~~ biological consumption in the OMZs,  
20 ~~which is associated with redistribution of DON. Our analyses demonstrate that weaker physical supply in the ETNP is the dominant process responsible for the asymmetry of the lower OMZs~~ whereas greater applying a reduced O:C utilization ratio leads to a large decrease in biological consumption ~~to the north plays a larger,~~ and a small decrease in physical supply. Our analyses suggest that biological consumption (greater rate to the south) cannot explain the asymmetric feature in the tropical Pacific OMZs, but physical processes (stronger supply to the south) play a major role in regulating the ~~upper~~ asymmetry of the  
25 tropical Pacific's OMZs. This study also highlights the ~~complex~~ roles of physical ~~supply~~ and biological ~~consumption~~ interactions/feedbacks in ~~shaping~~ contributing to the ~~asymmetric~~ asymmetry of OMZs in the tropical Pacific.

## 1 Introduction

Photosynthesis and respiration are important processes in all ecosystems on the Earth, with carbon and oxygen being the two main elements. The carbon cycle has garnered much attentions, ~~which made~~ with significant ~~progresses~~ progress in both the  
30 observations and modelling of biological processes (e.g., uptake of CO<sub>2</sub> and respiration), and physical/chemical processes (e.g.,

carbon fluxes between the atmosphere, land and ocean). However, the oxygen cycle has received much less attention despite its large role in the earth system (Breitburg et al., 2018; Oschlies et al., 2018).

~~Dissolved oxygen (DO) is a sensitive indicator of physical and biogeochemical processes in the ocean thus a key parameter for understanding the ocean's role in the climate system (Stramma et al., 2010). In addition to photosynthesis and respiration, the distribution of DO in the world's oceans is also regulated by air-sea gas exchange, ocean circulation and ventilation~~  
35 Dissolved oxygen (DO) is a sensitive indicator of physical and biogeochemical processes in the ocean thus a key parameter for understanding the ocean's role in the climate system (Stramma et al., 2010). In addition to photosynthesis and respiration, the distribution of DO in the world's oceans is also regulated by air-sea gas exchange, ocean circulation and ventilation  
40 (Bettencourt et al., 2015; Bopp et al., 2002; Levin, 2018). Unlike most dissolved nutrients that display an increase in concentration with depth, DO concentration is generally low at mid-depth of the ocean. The most remarkable feature in the oceanic oxygen dynamics is the so-called Oxygen Minimum Zone (OMZ) that is often present below 200 m in the open oceans (Karstensen et al., 2008; Stramma et al., 2008).  
45 . Previous studies have used the isoline of 20 mmol m<sup>-3</sup> as the boundary of the OMZ for the estimation of OMZ volume (Bettencourt et al., 2015; Bianchi et al., 2012; Fuenzalida et al., 2009), and also as an up limit to determine the suboxic water (Wright et al., 2012).

The world's two largest OMZs are observed in the Eastern Tropical North Pacific (ETNP) and South Pacific (ETSP), showing a peculiar asymmetric structure across the equator, i.e., a much larger volume of suboxic water (<20 mmol m<sup>-3</sup>) to the north  
50 than to the south (Bettencourt et al., 2015; Paulmier and Ruiz-Pino, 2009). It is known that OMZs are caused by the biological consumption associated with remineralization of organic matter (OM), and weak physical supply of DO due to sluggish subsurface ocean circulation and ventilation (Brandt et al., 2015; Czeschel et al., 2011; Kalvelage et al., 2015). Although there have been a number of observation-based analyses addressing the dynamics of OMZs in the tropical Pacific during the past decade (Czeschel et al., 2012; Garçon et al., 2019; Schmidtko et al., 2017; Stramma et al., 2010), our understanding is  
55 ~~uncompleted in terms of limited on~~ the underlying mechanisms that regulate DO dynamics at mid-depth ~~due to the limitation of available data~~ (Oschlies et al., 2018; Stramma et al., 2012).

Large-scale physical-biogeochemical models have become a useful tool to investigate the potential sensitivity of OMZs to climate change (Duteil and Oschlies, 2011; Ward et al., 2018; Williams et al., 2014). However, many models ~~still have some~~  
60 ~~difficulties in reproducing been unable to reproduce the~~ observed patterns of asymmetric OMZs in the tropical Pacific (Cabre et al., 2015; Shigemitsu et al., 2017), which may be due to “unresolved ocean transport processes, unaccounted for variations in respiratory oxygen demand, or missing biogeochemical feedbacks” (Oschlies et al., 2018); (Oschlies et al., 2018). A common problem is that the two asymmetric OMZs merge into one in most models ~~that often overestimate the~~ due to overestimated  
OMZ volume ~~of OMZs~~ in the tropical Pacific, which may be related to ~~weaker the regulation of~~ physical supply and/or higher

65 ~~rates of biological consumption/~~respiration demand (Cabre et al., 2015; Shigemitsu et al., 2017). Recent studies have also indicated that a realistic representation of circulation and ventilation processes with a high-resolution ocean model is critical to predict the asymmetric OMZs in the tropical Pacific (Berthet et al., 2019; Busecke et al., 2019). ~~Apparently~~Hence, it's necessary to carry out model-data integrative studies to improve model capacity of simulating the dynamics of the tropical OMZs, and to better understand ~~the~~ relative roles of physical and biological processes. ~~Without~~  
70 such process understandings, it is unclear a priori whether simply increasing resolution will render better simulations and predictions.

A basin-scale ocean general circulation model coupled with a dynamic marine ecosystem-carbon model (OGCM-DMEC) was developed for the tropical Pacific (Wang et al., 2008; Wang et al., 2015; Wang et al., 2009b), which showed capability of  
75 reproducing observed spatial and temporal variations of physical, nutrient and carbon fields in the upper ocean (Wang et al., 2008; Wang et al., 2015; Wang et al., 2009b), and nitrate, iron, POC/detritus and export production below 200 m (Yu et al., 2021). In this study, we conduct model sensitivity experiments and evaluation on responses of mid-depth DO to parameterizations of two relevant processes (i.e., oxygen-restricted remineralization and vertical mixing). We first carry out model calibration and validation using observational data of basin-scale DO and oxygen consumption ~~rate~~in the water column  
80 of the southern tropical Pacific to improve the simulation of OMZs in the tropical Pacific. Then, we ~~use the improved model to evaluate how~~analyse the impacts of new parameterizations on biological consumption and physical supply ~~regulate and their~~relative contributions to the dynamics of mid-depth DO. The objective of this study is to advance our model capacity to simulate the oceanic oxygen cycle, and to identify the mechanisms driving the asymmetric OMZs in the tropical Pacific.

## 2. Model description

### 85 2.1 Ocean physical model

The basin-scale OGCM, a reduced-gravity, primitive-equation, sigma-coordinate model, is coupled to an advective atmospheric model (Murtugudde et al., 1996). ~~There are 20 layers with variable thicknesses in the OGCM. The mixed layer (the upper-most layer) depth is determined by the Chen mixing scheme (Chen et al., 1994), which varies from 10 m to 50 m on the equator. The remaining layers in the euphotic zone are approximately 10 m in thickness. The model domain is between~~  
90 ~~30°S and 30°N, and zonal resolution is 1°. Meridional resolution varies between 0.3° and 0.6° over 15°S–15°N (1/3° over 10°S–10°N), and increases to 2° in the southern and northern “sponge layers” (the 25°–30° bands) where temperature, salinity, and nitrate are gradually relaxed back towards the observed climatological seasonal means from the World Ocean Atlas, 2013 (WOA2013; (Murtugudde et al., 1996). There are 20 layers with variable thicknesses and a total depth of ~1200 m in the~~  
95 ~~OGCM. The mixed layer (the upper-most layer) depth is determined by the Chen mixing scheme (Chen et al., 1994), which varies from 10 m to 50 m on the equator. The remaining layers in the euphotic zone are approximately 10 m in thickness. The vertical resolution is approximately 30–50 m in the core OMZ (at ~300–500 m). The model domain is between 30°S and 30°N~~

for the Pacific, and zonal resolution is 1°. Meridional resolution varies between 0.3° and 0.6° over 15°S-15°N (1/3° over 10°S-10°N), and increases to 2° in the southern and northern “sponge layers” (the 25°-30° bands) where temperature, salinity, nutrients and DO are gradually relaxed back towards the observed climatological seasonal means. The model closes the western boundary and no representation of the Indonesian throughflow is included. The boundary conditions of temperature, salinity, nitrate and DO are from the World Ocean Atlas, 2013 (WOA2013: <http://www.nodc.noaa.gov/OC5/woa13/pubwoa13.html>), and boundary condition for dissolved iron is based on limited field data, and given by a linear regression against temperature (see details in Christian et al., 2001). Such model configuration may have a disadvantage for longer simulations and analyses, but has the advantage in reproducing the spatial patterns of most physical and biogeochemical fields.

The model is forced by atmospheric conditions: climatological monthly means of solar radiation and cloudiness, and interannual 6-day means of precipitation and surface wind stress. Precipitation is from <ftp://ftp.cdc.noaa.gov/Datasets/gpcp>. Wind stresses are from the National Centers for Environmental Prediction (NCEP) reanalysis (Kalnay et al., 1996). Air temperature and humidity above the ocean surface are computed by the atmospheric mixed layer model. Initial conditions were obtained from outputs of an interannual hindcast simulation over 1948-1978-2000, which itself is initialized from a 30-year spin up with climatological run with a 30-year spin up forcing, followed by two 40-year interannual simulations. The initial conditions for the climatological spin up are specified from the WOA2013, iron concentration for the spin up was initialized from limited field data collected in the tropical Pacific (Johnson et al., 1997). We carry out an interannual simulation for the period of 1978-2018-2010, and analyse the mean states from model output for simulations over the period of 1981-2000-1991-2010.

## 2.2 Ocean biogeochemical model

~~The DMEC model is the main part of the biogeochemical model that is embedded in the basin-scale OGCM.~~ The DMEC model consists of eleven components: small (S) and large (L) sizes of phytoplankton ( $P_S$  and  $P_L$ ), zooplankton ( $Z_S$  and  $Z_L$ ) and detritus ( $D_S$  and  $D_L$ ), dissolved organic nitrogen (DON), ammonium, nitrate, dissolved iron, and DO (Figure 1). Phytoplankton growth is co-limited by nitrogen and iron, which is critical in the tropical Pacific. The model simulates the iron cycle using variable Fe:N ratios, and incorporates atmospheric iron input. All biological components use nitrogen as their unit, and in which sources/sinks are determined by biological and chemical processes in addition to the physical processes (circulation and vertical mixing) that are computed in a manner similar to physical variables by the OGCM.

In this model, net community production (NCP) is computed as:

$$-NCP = 6.625(\mu_S P_S + \mu_L P_L - r_S Z_S - r_L Z_L - c_{DON} DON - c_{D_S} D_S - c_{D_L} D_L) \quad (1)$$

~~where 6.625 is the C:N ratio,  $\mu$  the rate of phytoplankton growth,  $r$  the rate of zooplankton respiration,  $c$  the rates of detritus decomposition and DON remineralization. The equations for biogeochemical processes and model parameters are described in Appendix A and B. There have been changes in some parameters comparing with those in Wang et al. (2008), which were~~

130 based on our model calibration and validation for chlorophyll (Wang *et al.*, 2009a), nitrogen cycle (Wang *et al.*, 2009b) and carbon cycle (Wang *et al.*, 2015).

where 6.625 is the C:N ratio,  $\mu$  the rate constant of phytoplankton growth,  $r$  the rate constant of zooplankton respiration,  $c$  the rate constants of detritus decomposition and DON remineralization. The equations for biogeochemical processes and model parameters are given in Appendix A and B. There were changes in some parameters comparing with those in Wang *et al.* (2008), which were based on our model calibration and validation for chlorophyll (Wang *et al.*, 2009a), nitrogen cycle (Wang *et al.*, 2009b) and carbon cycle (Wang *et al.*, 2015).

135 Recently, we have made further improvements in the parameterizations of detritus decomposition and DON remineralization (eq. B21-B23), which result from the first round of model calibration on DO distribution using WOA2013. In brief,  $c_{DON}$  decreases with depth over 100-1000 m, following an exponential function in this study. The differences in the related parameters are given in Appendix C.

### 2.3 Computation of oxygen sources and sinks

The time evolution of DO is regulated by physical, biological and chemical processes:

$$\frac{\partial O_2}{\partial t} = -u \frac{\partial O_2}{\partial x} - v \frac{\partial O_2}{\partial y} - w \frac{\partial O_2}{\partial z} + O_{mix} - O_{bio} + O_{gas} \quad (2)$$

145 where  $u$ ,  $v$ , and  $w$  are zonal, meridional, and vertical velocity, respectively.  $O_{mix}$  is the vertical mixing term that is calculated by three subroutines. Briefly, the first one computes convection to remove instabilities in the water column, and the second one determines the mixed layer depth. The third one computes partial vertical mixing ( $K_z$ ) between two adjacent layers to relieve gradient Richardson ( $Ri$ ) number instability, which is calculated as follows:

$$K_z = \left(1 - \left(\frac{Ri}{0.7}\right)^\lambda\right) (Ri < 0.7) \quad (3)$$

$$150 \quad K_z = 0 (Ri \geq 0.7) \quad (4)$$

where the mixing parameter  $\lambda$  is set to 1. Clearly, partial vertical mixing is the dominant process influencing physical supply of DO in the intermediate waters.

The biological source/sink term  $O_{bio}$  is computed as follows:

$$155 \quad -O_{bio} = 1.3NCP R_{OC} NCP \quad (5)$$

where  $1.3R_{OC}$  is the O:C utilization ratio (set to 1.3 in reference simulation, according to the Redfield ratio-). Below the euphotic zone, DO concentration is determined by physical supply and biological consumption that results from detritus decomposition and DON remineralization, in which DON remineralization is dominant because DON ~~pool~~ is several times greater than detritus (Wang *et al.*, 2008)(Wang *et al.*, 2008).

The flux of  $O_2$  from the atmosphere to the surface ocean is computed as:

$$O_{gas} = (O_{sat} - O)K_0 \quad (6)$$

165 where  $O_{sat}$  is the  $O_2$  saturation, a function of temperature and salinity (~~Weiss, 1970~~)(Weiss, 1970), and  $K_0$  the gas transfer velocity that is a function of wind speed ( $u_s$ ) and SST according to Wanninkhof (1992):

$$K_0 = 0.31u_s^2 \sqrt{\frac{S_c}{S_c20}} \sqrt{\frac{S_c}{S_c20}} \quad (7)$$

where  $S_c$  and  $S_{c20}$  are the Schmidt number at SST and 20° C, respectively:

$$S_c = 1953 - 128T + 3.99T^2 - 0.05T^3 \quad (8)$$

### 3. Model experiments ~~and validation~~

#### 170 3.1 Evaluation of DO distribution from the reference run

We first evaluate simulated DO for the tropical Pacific Ocean using the outputs from OGCM-DMEC V1.2 (hereafter reference run). ~~We focus on model data comparisons over 200-400 m, 400-700 m and 700-1000 m, which use the same set of parameters as Yu et al. (2021). We focus on model-data comparisons over 200-400 m, 400-700 m and 700-1000 m, that broadly represent the upper OMZ, lower OMZ and beneath OMZ, respectively. The WOA2013 data shows a much larger area of suboxic waters (<20 mmol m<sup>-3</sup>) in the ETNP than in the ETSP over 200-400 m and 400-700 m (Figure 2a and 2c), but no suboxic water over 700-1000 m (Figure 2e). Although the reference run produces two OMZs off the equator over 200-400 m (Figure 2b), the sizes of suboxic water are much larger in the reference run than those in the WOA2013 data. The reference run significantly over-estimate~~estimates the size of suboxic water and underestimates DO concentration over 400-700 m (Figure 2d). The difference between WOA2013 and the reference run is small over 700-1000 m, except in the eastern tropical Pacific (Figure 2f). ~~The relative roles of the physics vs. the biogeochemistry in determining the bias are diagnosed further below.~~

175  
180

#### 3.2 Sensitivity experiments

~~Given~~There have been advances in understanding of oxygen consumption. For example, recent studies have showed that ~~the mid-depth DO concentration is influenced by physical supply and biological consumption, O:C utilization ratio varies largely across different basins, e.g., from 0.6 to 2.1 in the Pacific (Moreno et al., 2020; Tanioka and Matsumoto, 2020), and rates of DOM remineralization of DON is the dominant process for or~~ oxygen consumption, ~~the underestimated DO are influenced by oxygen level, i.e., a reduction under low DO conditions (Beman et al., 2020; Bertagnolli and Stewart, 2018; Sun et al., 2021). Based on the field data at mid-depth would be a result of overestimation of (~350 m) in the Peruvian OMZ (Kalvelage et al., 2015), we derive a kinetics function between oxygen consumption associated with DON remineralization and/or~~ underestimation of supply. ~~Indeed, rate and DO concentration, which yields the reference run over estimates biological~~

185  
190

consumption over 100–400 m half saturation constant  $K_m$  being 6.9 and 18.7  $\text{mmol m}^{-3}$  (Figure 3). Thus, we apply a ~~By adding this functional form to equation 5, one would get a varying and also reduced DON remineralization constant (50% of the reference run), which leads to a remarkable improvement in simulated DON and consumption. O:C utilization ratio, with lower ratios in in low-DO waters.~~

195

The reference run ~~applies~~ applied a zero value for background diffusion. However, a previous modelling study ~~has demonstrated that vertical background diffusion is~~ was an important process for DO supply at mid-depth (Duteil and Oschlies, 2011)(Duteil and Oschlies, 2011). Accordingly, we conduct a few more simulations (Table 4S1) to investigate how ~~reducing remineralization rate and applying different values for vertical~~ a reduced O:C utilization ratio (setting  $K_m$  as 6.9 and 18.7  $\text{mmol m}^{-3}$ ) and adding background diffusion (setting  $K_b = 0.1, 0.3, 0.5$  and  $0.5 \text{ cm}^2 \text{ s}^{-1}$ ) affect the simulated DO distribution and ~~asymmetric~~ asymmetry of OMZs in the tropical Pacific. ~~Changing~~ To eliminate complex interactions and feedbacks, the ~~intensity~~ addition of ~~vertical~~ background diffusion ~~has relatively small influence on vertical distributions of DON and DO consumption in the OMZ (is only applied to the key variables (DO and DON) in this study.~~

200

205

Figure 3).

~~We then compare simulated DO and WOA2013 climatology data. Figure 4a4 illustrates that based on WOA2013 database, there is a larger volume of suboxic water located north of  $\sim 5^\circ\text{N}$  and a smaller volume of suboxic water over  $12^\circ\text{S}$ – $4^\circ\text{S}$ , which are separated by relatively higher DO ( $>30$   $\text{mmol m}^{-3}$ ) water along the equator. Both Cd0.5 run (Figure 4e) and the reference run (Figure 4b) produce much larger volumes of suboxic water that are extend to the equatorial region, and even merge into one. Clearly, there~~ There is an improvement in simulated DO with reduced O:C utilization ratio (Figure 4b and 4c) and enhanced vertical mixing (Figure 4d and 4h). Clearly, combination of reduced O:C utilization ratio and enhanced vertical mixing leads to a further improvement in simulated mid-depth DO (Figure 4e, 4f, 4i and 4j). In particular, the combination of a stronger background diffusion (Figure 4d, 4e and 4f). Overall, Cd0.5Kb0.5 is able to capture with a smaller O:C utilization ratio (i.e., the  $K_m 18.7 K_b 0.5$  run) results in the best simulation that reproduces the observed spatial distribution of mid-depth DO, especially the asymmetric feature (i.e., a larger volume of suboxic water to the north but a smaller size of suboxic water to the south), and relatively higher DO ( $\sim 30$ – $40 \text{ mmol m}^{-3}$ ) over  $2^\circ\text{S}$ – $2^\circ\text{N}$ ).

210

215

### 3.3 Model validation

220

To further evaluate the performance of experiments, ~~three~~ a few statistical measures are applied over 200–400 m, 400–700 m and 700–1000 m in the ETNP ( $165^\circ\text{W}$ – $90^\circ\text{W}$ ,  $5^\circ$ – $20^\circ\text{N}$ ) and ETSP ( $110^\circ\text{W}$ – $80^\circ\text{W}$ ,  $10^\circ\text{S}$ – $3^\circ\text{S}$ ). As shown in Table 21, compared ~~to~~ with the reference run, bias, MAE and root mean square error (RMSE) are reduced in all ~~decrease in the new experiments~~ simulations, with the smallest values from Cd0.5Kb0.5 run except over 700–1000 m in the ETNP. For



example, both MAE and bias are lowest from Cd0.5Kb0.5 in the Km18.7Kb0.5 run are smallest over 200-700 m in the ETNP ( $6.95-16.44 \text{ mmol m}^{-3}$ ) ( $<7.8$  and over 200-1000 m in ETSP ( $3.12-7.59$ )  $10.2 \text{ mmol m}^{-3}$ ). Many current models show much large RMSE ( $\sim 20-80 \text{ mmol m}^{-3}$ ) with respect to observed DO from mixed layer to 1000 m (Cabre *et al.*, 2015; Bao and Li, 2016) (Bao and Li, 2016; Cabre *et al.*, 2015). Figure 5 also illustrates that Cd0.5Kb0.5 the Km18.7Kb0.5 run produces the best outputs, with the largest correlation coefficients (0.77-0.94) and also the smallest distance to 1 in normalized standard deviation (0.54-1.81 in ETNP and 0.33-1.63 in ETSP).

We also compare the sizes of suboxic water and hypoxic water between model simulations and WOA2013 (Table 32). Based on WOA2013, we estimate that the sizes of suboxic water and hypoxic water are  $5.97 \times 10^{15} \text{ m}^3$  and  $19.98 \times 10^{15} \text{ m}^3$  in the north, and  $1.43 \times 10^{15} \text{ m}^3$  and  $7.12 \times 10^{15} \text{ m}^3$  in the south, respectively. While the Cd0.5 run (with a reduced remineralization rate) results in O:C utilization ratio and enhanced vertical mixing can lead to an improvement in simulated OMZ volume, a significant improvement is obtained with the combination of reduced remineralization O:C utilization ratio and enhanced vertical mixing (i.e., with background diffusion). Overall, the Km18.7Kb0.5 simulation has the best performance for reproducing the OMZ volume is Cd0.5Kb0.5 simulation that predicts volumes, showing similar volumes for the suboxic water ( $6.61 \times 10^{15}$   $5.55 \times 10^{15} \text{ m}^3$  to the north and  $1.56 \times 10^{15}$   $12 \times 10^{15} \text{ m}^3$  to the south) and the hypoxic water ( $19.62 \times 10^{15}$   $20.91 \times 10^{15} \text{ m}^3$  and  $7.13 \times 10^{15}$   $39 \times 10^{15} \text{ m}^3$ ).

We then use cruise data to further validate the modelled DO from the best run (Cd0.5Kb0.5 Km18.7Kb0.5), using the time series of the observed DO data (<https://cchdo.ucsd.edu/>). Figure 6 shows illustrates that the model can generally reproduce the vertical-zonal distribution distributions of DO along  $10^\circ\text{N}$  and  $17^\circ\text{S}$ , spanning from 1989 to 2009, particularly in the eastern tropical Pacific. For example, cruise data from the P04 line during April-May, 1989 show a large area of low DO water spanning from  $\sim 200$  m to  $\sim 800$  m (Figure 6a), and our model also predicts low DO water over  $\sim 200-700$  m (Figure 6b).

#### 4 Model evaluation results and discussions

In this section, we further compare the improved model simulations (Cd0 Km18.7, Kb0.5 and Cd0.5Kb0 Km18.7Kb0.5) with the reference run to diagnose the relative contributions influences of improved parameterizations on the distribution of mid-depth DO, and biological consumption and physical supply to the asymmetric OMZs in the tropical Pacific, aiming to identify. We then analyse the interactions of physical and biogeochemical processes, and the impacts on the source and sink for the mid-depth DO. In the end, we explore the underlying mechanisms regulating the dynamics of mid-depth DO asymmetry of OMZs in the tropical Pacific.



#### 4.1 Changes of mid-depth DO due to reduced remineralization-O:C utilization ratio and enhanced vertical mixing

255 We first compare the changes of in DO concentration concentrations between the three model simulations simulations over 200-400 m, 400-700 m, and 700-1000 m (Figure 7). Clearly, applying a reduced remineralization rate largely O:C utilization ratio causes an increase mid-depth of DO in all three layers, with a greater the greatest increase ( $-0.22 (>6 \text{ mmol m}^{-3})$  over in the 200-400 m layer (Figure 7a), followed by a modest increase ( $-0.3-6 \text{ mmol m}^{-3}$ ) over 400-700 m (Figure 7d), and a small). Although DO increase ( $0.3 \text{ mmol m}^{-3}$ ) over is generally smaller in the 700-1000 m layer (Figure 7h),) than in the 400-700 m layer (Figure 7d), the increase is greater in the north OMZ over 700-1000 m than over 400-700 m. Enhanced vertical mixing -results in a small increase of DO ( $\sim 2.5 \text{ mmol m}^{-3}$ ) in DO (the  $10 \text{ mmol m}^{-3}$  S-10°N band over 200-400 m (Figure 7b)), but a large increase ( $\sim 5-12.15 \text{ mmol m}^{-3}$ ) in majority of the basin over 400-700 m and 700-1000 m (Figure 7e and 7i). A number of modelling studies have demonstrated that parameterization of vertical mixing has significant impacts on the mean state of DO distributions at

265 Overall, the mid-depth (Duteil and Oschlies, 2011; Gnanadesikan *et al.*, 2013) DO shows an increase with the combination of a reduced O:C utilization ratio and enhanced vertical mixing (Figure 7c, 7f & 7j). A great increase of DO ( $>15 \text{ mmol m}^{-3}$ ) occurs in majority of the basin over 400-700 m, mainly in the central tropical Pacific over 200-400 m, but in a few small areas over 700-1000 m. The spatial pattern and magnitude of DO increase resulting from the combination of reduced O:C utilization ratio and enhanced vertical mixing, have a large similarity to those with reduced O:C utilization ratio for the 200-400 m layer (Figure 7a), but to those under enhanced vertical mixing below 400 m (Figure 7e & 7i). For example, the relative increase of DO is similarly larger in the northern OMZ over 200-400 m under a reduced O:C utilization ratio with and without the addition of background diffusion, and over 700-1000 m under enhanced vertical mixing (i.e., with additional background diffusion) with and without the change in the O:C utilization ratio. Our analyses suggest that the dominant process regulating the DO

270 dynamics is biological consumption over 200-700 m, but physical supply over 400-1000 m.

280 We also assess the response of mid-depth DO to the combination of reduced remineralization rate and enhanced vertical mixing (Cd0.5Kb0.5 minus reference run). Overall, the increase of DO is greater over 200-400 m ( $-10.24 \text{ mmol m}^{-3}$ ) than over 400-700 m ( $-8.18 \text{ mmol m}^{-3}$ ) and 700-1000 m ( $-6.12 \text{ mmol m}^{-3}$ ) (Figure 7c, 7f & 7j). The spatial pattern and magnitude of increased DO resulted from the combined changes of remineralization rate and vertical mixing have a large similarity to those caused by reduced remineralization rate for the 200-400 m layer (Figure 7a), but are similar to those due to enhanced mixing below 400 m (Figure 7d & 7h). Our analyses indicate that DO dynamics is regulated by biological processes above 400 m, but by physical processes over 400-1000 m. The larger biological influence on the upper OMZ is attributable to the greater rate of DO consumption (Karstensen *et al.*, 2008) whereas the greater physical impact on the lower OMZ reflects the relatively larger

285 role of supply than consumption.

#### **4.2 Responses of 4.2 Effects of reduced O:C utilization ratio and enhanced vertical mixing on consumption and supply to reduced remineralization and enhanced mixing**

~~We then~~ To better understand the effects of changes in the biological and/or physical parameters on the DO dynamics, we then evaluate the ~~changes~~responses of biological consumption and physical supply ~~of DO due to reduced remineralization and/or enhanced mixing. Reducing remineralization rate by 50% (Cd0.5 minus reference) leads to.~~ As illustrated in Figure 8, changes in biological consumption are almost identical under a reduced O:C utilization ratio with or without background diffusion. In particular, biological consumption shows a large decrease (~~~1.5-2.0~~~0.8 mmol m<sup>-3</sup> yr<sup>-1</sup>) over 200-400 m, ~~modest~~ (Figure 8b), and a small decrease (~~~0.2-1.0~~~0.5 mmol m<sup>-3</sup> yr<sup>-1</sup>) over 400-700 m ~~and small decrease (~0.2, with the largest decrease in the northern OMZ (Figure 8e); there is a very small change in biological consumption over 700-1000 m, i.e., a decrease of <0.1-0.2 mmol m<sup>-3</sup> yr<sup>-1</sup>) over 700-1000~~ majority of the basin but an increase of <0.1 mmol m<sup>-3</sup> yr<sup>-1</sup> in some parts of subtropical region (Figure 8a, 8d and 8h8j). On the other hand, enhanced vertical mixing ~~causes much greater increase of supply over 400-1000 m than over 200-400 m.~~ leads to a small increase (<0.2 mmol m<sup>-3</sup> yr<sup>-1</sup>) in biological consumption in all three layers, with a relatively larger increase in the northern OMZ (Figure 8c, 8f and 8j).

Figure 9 shows the effects of a reduced O:C utilization ratio and enhanced vertical mixing on physical supply. With the combination of a reduced O:C utilization ratio and enhanced vertical mixing, physical supply shows a small increase (by ~~~0.2-1.0~~~0.2-1.0 mmol m<sup>-3</sup> yr<sup>-1</sup>) in the whole basin over 700-1000 m (Figure 9h) and only outside the OMZs over 400-700 m (Figure 9d), but a relatively larger decrease in the OMZs over 200-700 m (by ~~~0.2-6~~~0.2-6 mmol m<sup>-3</sup> yr<sup>-1</sup>) (Figure 9a and 9d). Clearly, enhanced vertical mixing leads to an increase of physical supply over majority of the basin, with greater increase over 400-1000 m (~~~0.2-1.0~~~0.2-1.0 mmol m<sup>-3</sup> yr<sup>-1</sup>) than over 200-400 m (~~~0.4~~~0.4 mmol m<sup>-3</sup> yr<sup>-1</sup>) (Figure 9c, 9f and 9j). However, applying a reduced O:C utilization ratio causes a large decrease of physical supply above 700 m, with greater decrease over 400-700 m in the OMZs (~~~0.2-6~~~0.2-6 mmol m<sup>-3</sup> yr<sup>-1</sup>), and very small changes (<0.2 mmol m<sup>-3</sup> yr<sup>-1</sup>) over 700-1000 m (Figure 9b, 9e and 9i). Overall, rate of physical supply is largely determined by vertical mixing over 700-1000 m, by both vertical mixing and biological consumption over 400-700 m, but by consumption over 200-400 m, implying complex physical-biological interactions and feedbacks in the tropical Pacific OMZs.

#### **4.3 Interactive effects of physical and biological processes on source and sink of mid-depth DO**

There is evidence that enhanced mixing can have large influences not only on physical processes (e.g., the strength of water mixing) but also on biological processes (e.g., transport of organic materials), which have direct or indirect effects on the evolution of mid-depth DO (Andrews et al., 2017; Duteil and Oschlies, 2011; Stramma et al., 2012). Our analyses show an increase in physical supply under enhanced vertical mixing in most parts of the 200-1000 m layer in the eastern tropical Pacific (over 120°W-90°W) (Figure 10). Interestingly, the greater increase (>1 mmol m<sup>-3</sup> yr<sup>-1</sup>) is below the OMZs over 15°S-10°N using 1.3 as the O:C utilization ratio (Figure 10a), but occurs over a much larger area (i.e., over 15°S-20°N) and within the OMZs using a reduced (and also varying) O:C utilization ratio (Figure 10d). Enhanced vertical mixing also results in a

320 generally small increase in biological consumption, with greater increases in OMZs using a reduced O:C utilization ratio  
(Figure 10e) than using a constant Redfield ratio of 1.3 (Figure 10b). The small increase in consumption outside of OMZs is  
largely attributable to increased DON concentration (data not shown) that results from the enhanced vertical mixing whereas  
the increase of consumption inside the OMZs would be a result of the interactions and feedbacks of various physical, biological  
and chemical processes. Clearly, there is an overall increase in net flux, with the largest increases occurring mainly outside the  
325 OMZs (Figure 10c and 10f).

To further investigate the interactive effects of a reduced O:C utilization ratio and enhanced mixing, we then compare the  
responses of biological consumption and physical supply to changes in the O:C utilization ratio with and without background  
diffusion (Figure 11). While a reduced O:C utilization ratio can result in a decrease in consumption above 600 m, the decrease  
330 is slightly less in the OMZs with background diffusion (Figure 11d) than without background diffusion (Figure 11a). Similarly,  
physical supply also shows a decrease in the OMZs under a reduced O:C utilization ratio (Figure 11b), with a lesser decrease  
under the addition of background diffusion (Figure 11e). The greatest difference is found in the core OMZs for both biological  
consumption (Figure 11h) and physical supply (Figure 11i), but larger differences are found in supply. A previous modeling  
study also demonstrates that physical contribution to the changes of DO is much greater than biogeochemical contribution  
335 (Montes et al., 2014). However, a reduced O:C utilization ratio results in a clear increase in net flux in the whole water column  
over 200-1000 m, with a great increase above the core OMZs within the 10°S-10°N band (Figure 11c and 11f).

Physical supply could be divided into horizontal advection, vertical advection, and vertical mixing. Our model performs well  
in simulating the meridional and zonal advectons, and vertical mixing processes of DO transport (see Figure S2), which allows  
340 us to evaluate the responses of different supply components to the reduced O:C utilization ratio. As shown in Figure 12, there  
is no clear pattern in the responses of advective supply, with very small values ( $< \sim 1 \text{ mmol m}^{-3} \text{ yr}^{-1}$ ) over the entire basin  
(Figure 12h and 12i). However, the DO supply by vertical mixing shows a strong response, with similar patterns to those of  
total supply and a large decrease in the suboxic waters (Figure 12c and 12f). While applying a reduced O:C utilization ratio  
causes a decrease in the DO supply ( $\sim 1\text{-}6 \text{ mmol m}^{-3} \text{ yr}^{-1}$ ) by vertical mixing, the decrease is larger in the OMZs without the  
345 addition of background diffusion. On the other hand, there is an increase in the supply by vertical mixing below the OMZs  
under a reduced O:C utilization ratio, in particular with the addition of background diffusion (Figure 12f). The largest  
difference ( $\sim 1\text{-}2 \text{ mmol m}^{-3} \text{ yr}^{-1}$ ) is found within the hypoxic waters (Figure 12j), which reflects the strong feedback between  
physical and biological processes in the OMZs.

350 There is evidence that the physical and biogeochemical processes have multiple interactions with impacts on various physical,  
chemical and biological fields and implications for DO dynamics (Breitburg et al., 2018; Duteil and Oschlies, 2011; Oschlies  
et al., 2018). For example, observational and modelling studies show that changes in vertical mixing intensity can affect the  
distributions of organic matter thus oxygen consumption at mid-depth (Duteil and Oschlies, 2011; Talley et al., 2016), and

vertical distributions of DOM concentration and its remineralization around the OMZ in turn can alter the intensity of vertical mixing for DO (Loginova et al., 2019). Recent studies have demonstrated that a changing O:C utilization ratio (or respiration quotient) has various impacts on biological and chemical processes, with an impact on microbial respiration thus oxygen consumption (Moreno et al., 2020; Tanioka and Matsumoto, 2020). In particular, applying a smaller O:C utilization ratio leads to lower consumption rates, thus higher DO levels (Moreno et al., 2020), which would have large effects on DO gradients thus vertical mixing particularly in low-DO waters (e.g., in the OMZs).

#### **4.4 Impacts of biological and physical processes on asymmetric OMZs**

There is evidence of asymmetric features in many biogeochemical parameters in the tropical Pacific. For example, POC flux at 500 m is greater in the northern tropical Pacific ( $\sim 4 \text{ mmol C m}^{-2} \text{ d}^{-1}$ ) (Van Mooy et al., 2002) than in the southern tropical Pacific ( $< 1 \text{ mmol C m}^{-2} \text{ d}^{-1}$ ) (Pavia et al., 2019). Similarly, our regional model reproduces an asymmetric pattern for POC flux, with larger values to the north than to the south. Field studies have reported an asymmetry in DOM distribution over  $\sim 200$ - $1000 \text{ m}$  in the central-eastern tropical Pacific, i.e., higher levels of DON and DOC to the north than to the south (Hansell, 2013; Libby and Wheeler, 1997; Raimbault et al., 1999). Our model simulation also reveals an asymmetric DON at mid-depth, i.e.,  $\sim 6$ - $7 \text{ mmol m}^{-3}$  in the ETNP and  $\sim 4$ - $5 \text{ mmol m}^{-3}$  in the ETSP (data not show). However, an earlier field study reported higher rates of organic carbon remineralization over  $200$ - $1000 \text{ m}$  to the south ( $\sim 2$ - $10 \text{ mmol m}^{-3} \text{ yr}^{-1}$ ) than to the north ( $\sim 1$ - $6 \text{ mmol m}^{-3} \text{ yr}^{-1}$ ) in the eastern/central tropical Pacific (Feely et al., 2004). Similarly, our model simulation also shows such asymmetric feature of biological consumption below  $200 \text{ m}$  in the tropical Pacific, i.e.,  $\sim 2$ - $8 \text{ mmol m}^{-3} \text{ yr}^{-1}$  in the ETSP and  $\sim 1$ - $6 \text{ mmol m}^{-3} \text{ yr}^{-1}$  in the ETNP.

It appears that the asymmetric distributions differ largely between biological parameters, and there are almost opposite patterns between oxygen consumption (or DOM remineralization) and DOM concentration. This discrepancy may be attributed to the rates of DOM remineralization in the water column, which is determined not only by DOM concentration, but also by the stoichiometry associated with microbial respiration (Wang et al., 2008; Zakem and Levine, 2019). Recent studies on respiration quotient demonstrate that the O:C utilization ratio is lower to the north than to the south in the tropical Pacific (Tanioka and Matsumoto, 2020; Wang et al., 2019), which primarily reflects the difference in oxygen limitation on microbial respiration (Kalvelage et al., 2015). Apparently, such asymmetry in biological consumption cannot explain the asymmetry in the tropical Pacific OMZs (i.e., lower DO levels to the north than to the south), indicating that other processes are responsible for the asymmetry.

Numerous studies have indicated that physical mixing is the only source of DO for the tropical OMZs (Czeschel et al., 2012; Brandt et al., 2015; Talley et al., 2016) (Brandt et al., 2015; Czeschel et al., 2012; Duteil et al., 2020). For example, turbulent background-diffusion accounts is argued to account for 89% of the net DO supply for the core OMZ layer of south tropical Pacific (Llanillo et al., 2018) (Llanillo et al., 2018). Figure 8e and 8i illustrate that physical supply is increased by  $\sim 0.2$ - $0.6$

390  $\text{mmol m}^{-3}\text{-yr}^{-1}$  in most of the mid-waters, with the largest increase in the southern part of central equatorial Pacific over 400–700 m. However, there is somehow a small decrease of physical supply in the ETNP over 200–400 m (by  $-0.03 \text{ mmol m}^{-3}\text{-yr}^{-1}$ , Figure 8b) and 400–700 m ( $<0.02 \text{ mmol m}^{-3}\text{-yr}^{-1}$ , Figure 8e), implying that increased DO under enhanced vertical mixing may be attributable to changes in biological consumption. There is evidence that larger-scale mass transport due to circulation and ventilation is more efficient in the south Pacific than in the north Pacific (Kuntz and Schrag, 2018), and the transit time from the surface to the OMZ is much longer in the ETNP than in the ETSP (Fu et al., 2018). Both our analyses and other modeling studies (Duteil, 2019; Shigemitsu et al., 2017) demonstrate that DO supply via vertical mixing is much weaker in the northern OMZ than in the southern OMZ in the tropical Pacific. All these analyses indicate that physical processes play a major role in shaping the asymmetry of the OMZs over the tropical Pacific.

400 We further compare biological consumption between Cd0.5Kb0.5 and the Cd0.5. Interestingly, enhanced vertical mixing results in a decrease in consumption, with the largest decreases ( $-0.03\text{--}0.07 \text{ mmol m}^{-3}\text{-yr}^{-1}$ ) over 400–700 m (Figure 8f), the smallest decrease ( $-0.01\text{--}0.04 \text{ mmol m}^{-3}\text{-yr}^{-1}$ ) over 200–400 m (Figure 8e) and modest decrease of  $-0.02\text{--}0.04 \text{ mmol m}^{-3}\text{-yr}^{-1}$  over 700–1000 m (Figure 8j). For the northern OMZ, biological consumption decreases by  $-0.03\text{--}0.07 \text{ mmol m}^{-3}\text{-yr}^{-1}$  over 200–700 m (Figure 8e and 8f), which is larger than the decreased rate ( $-0.01\text{--}0.03 \text{ mmol m}^{-3}\text{-yr}^{-1}$ ) of physical supply (Figure 8b and 8e).

#### 405 Remineralization rate of DOM in the ocean is determined by the size of DOM pool and temperature 4.5 Implications and limitations of the current research

410 There are inter-dependencies between the physical and biogeochemical processes (Wang *et al.*, 2008; Brewer and Peltzer, 2016)(Duteil and Oschlies, 2011; Gnanadesikan *et al.*, 2012; Niemeier *et al.*, 2019). Given that there is little difference ( $<10^{\circ}\text{C}$ ) in seawater temperature between different model experiments, the reduced consumption rates due to DOM remineralization would be a result of a smaller amount of DOM. Here, we evaluate the zonal and meridional distributions of DON together with remineralization rate. As shown in Figure 9a–9d, modelled consumption decreases from  $8 \text{ mmol m}^{-3}\text{-yr}^{-1}$  in the euphotic zone to  $1\text{--}2 \text{ mmol m}^{-3}\text{-yr}^{-1}$  below 400 m, and modelled DON decreases from  $5\text{--}8 \text{ mmol N m}^{-3}$  near the surface to  $1\text{--}4 \text{ mmol N m}^{-3}$  over 400–1000 m. Limited field studies reported that surface DON concentration was  $5\text{--}7 \text{ mmol N m}^{-3}$  in the ETSP (Loginova *et al.*, 2019), and consumption rate ranged from  $8.3 \text{ mmol m}^{-3}\text{-yr}^{-1}$  at  $\sim 200$  m to  $<3.1 \text{ mmol m}^{-3}\text{-yr}^{-1}$  below 500 m in the subtropical North Pacific, which may have influences on the asymmetry of OMZs in the tropical Pacific. Our study shows that rate of physical supply is sensitive to changes in both physical and biological parameterizations, particularly in low-DO waters. Since the physical contribution exceeds the biological contribution to mid-depth DO in the tropical Pacific (Llanillo *et al.*, 2018; Montes *et al.*, 2014), and the physical processes are more dominant in the ETSP, one may expect that physical-biological feedbacks are stronger to the south, which can lead to relatively larger net flux into the south OMZ.

420 Physical and biogeochemical interactions are complex over space, which have direct and indirect effects on the source and  
sink of DO (Sonnerup *et al.*, 2013)(Levin, 2018; Oschlies *et al.*, 2018), which are comparable to our model results. Our model  
simulations indicate that enhanced vertical mixing leads to a redistribution of DON below 200 m, with a decrease in DON  
concentration (0.06–0.12 mmol N m<sup>-3</sup>) over 600–900 m, but an increase (<0.04 mmol N m<sup>-3</sup>) below 1000 m in the eastern  
tropical Pacific (Figure 9h, 9i and 9j).

425 4.3 Impacts of biological consumption and physical supply on asymmetry of OMZs

Previous studies have demonstrated meridional asymmetric features in many physical and biological fields in the tropical  
Pacific, e.g., temperature and salinity (Fiedler and Talley, 2006), circulation and ventilation. On the one hand, supply of DO  
is greater under stronger physical transport in the south tropical Pacific. On the other hand, stronger physical processes can  
430 also lead to higher levels of nutrients and biological production and thus enhanced export production and oxygen consumption  
at mid-depth (Duteil and Oschlies, 2011), which can offset the rate of physical supply. In addition, stronger physical processes  
can also result in strengthened transport of DO and OM out to other regions (Kessler, 2006; Kuntz and Schrag,  
2018)(Gnanadesikan *et al.*, 2012; Yu *et al.*, 2021), which has complex impacts on DO balance in the southern OMZ.

435 There is evidence of strong interactions and feedbacks between carbon, nitrogen and carbon oxygen cycles in marine ecosystem.  
Limited studies indicate that O:C:N utilization ratios during microbial respiration vary largely in the water column (Libby and  
Wheeler, 1997; Wang *et al.*, 2009b)(Moreno *et al.*, 2020; Zakem and Levine, 2019), which may be largely associated with the  
asymmetries in water mass exchange between the equatorial and off-equator Pacific Ocean, and nitrogen cycling (e.g.,  
oxidation, nitrification and denitrification) not only has impacts on oxygen consumption/production but also is influenced by  
440 the oxygen level (Kug *et al.*, 2003)(Beman *et al.*, 2021; Kalvelage *et al.*, 2013; Oschlies *et al.*, 2019; Sun *et al.*, 2021).  
Accordingly, one may assume that the hemisphere asymmetry of OMZs could be related to the differences in physical supply  
and biological consumption between the ETNP and ETSP.

There is evidence that the size of tropical OMZ is largely influenced by biological processes, such as organic matter export  
and oxygen consumption (Keller *et al.*, 2016; Cavan *et al.*, 2017). Figure 10a illustrates that DO is increased in both ETNP  
445 and ETSP over 200–1000 m when remineralization rate decreases by 50%. The increase of DO is generally greater in the ETSP  
than in ETNP, except in the core OMZ (~300–500 m). Earlier field studies have revealed that DON concentration is much  
higher to the north than to the south in the central-eastern tropical Pacific (Libby and Wheeler, 1997; Raimbault *et al.*, 1999).  
Later studies showed that rates of DOM remineralization and/or oxygen consumption are also greater at mid-depth in the  
450 ETNP than in the ETSP (Feely *et al.*, 2004; Tian *et al.*, 2014; Kalvelage *et al.*, 2015), indicating that biological processes  
play a big role in determining the asymmetry of upper OMZs.

Recent studies also emphasized the role of changes in physical processes for the observed asymmetric OMZs in the tropical oceans. For instance, there is evidence that larger scale mass transport related to circulation and ventilation in the southern hemisphere is more efficient than in the northern hemisphere (Kuntz and Schrag, 2018), and the transit time from the surface to the OMZ is much longer in the ETNP than in the ETSP (Sonnerup *et al.*, 2013; Fu *et al.*, 2018). Clearly, our model experiment shows that enhanced vertical mixing leads to a significant increase in DO concentration below 200 m (Figure 10b). The increase of DO is similar below 1000 m in the ETNP and ETSP, but differs largely between the two regions, with much greater values over 200–1000 m in the ETSP. Our analysis indicates that enhanced vertical mixing increases the physical supply of DO over most of the water column, except over 300–500 m in the ETNP showing a small decrease (Figure 10c). The increase of supply is greater over 200–1000 m in the ETSP than in the ETNP, and significant increases ( $>0.2 \text{ mmol m}^{-3} \text{ yr}^{-1}$ ) are below 600 m (500 m) in the ETNP (ETSP). These analyses indicate that physical transport may be largely responsible for the asymmetry of lower OMZs.

. However, little attention has been paid to understand the coupling of carbon and oxygen cycles. It should be noted that the available data are also not sufficient for the parameterizations of relevant processes, which has hampered our ability to assess the impacts of biogeochemical processes associated with the nitrogen cycle on oxygen fields. Future observational and modelling studies are needed not only to improve our knowledge on the coupling of carbon, nitrogen and oxygen cycles in the ocean, but also to advance our understanding on the physical and biogeochemical interactions and feedbacks associated with the marine stoichiometry.

## 5. Conclusion

This paper describes an evaluation and validation of, we use a fully coupled basin-scale model (OGCM DMEC V1.2), focusing on the sensitivity of the asymmetric OMZs in the tropical Pacific to different investigate the impacts of parameterizations of vertical mixing and DOM remineralization on the dynamics of mid-depth DO, and vertical mixing analyse the underlying mechanisms for asymmetric OMZs in the tropical Pacific. Our results show study shows that the improved model with enhanced vertical mixing combined with reduced remineralization successfully reproduces is capable of reproducing the observed DO distributions and asymmetric OMZs in the tropical Pacific.

Our results demonstrate that reduced remineralization rate leads to remarkable decrease of biological consumption over 200–400 m, which largely affects with the distribution of DO in the upper OMZ. On the other hand, combination of enhanced vertical mixing and reduced O:C utilization ratio that causes an increase in DO concentration (or net flux) at mid-depth. Overall, enhanced vertical mixing causes makes a significant greater contribution to the increase over 400–1000 m, and the contribution from reduced O:C utilization ratio is greater over 200–700 m.



485 ~~Our analyses demonstrate that there is a large increase in physical supply of DO over 400–1000 m. Apart from the direct impact on physical supply, and a small increase in biological consumption under enhanced vertical mixing also results in the, and the increase in consumption is a result of redistribution of DOM in the water column, i.e., an increase over 200–1000 m and a decrease below 1000 m, leading to lower consumption in the OMZs.~~

490 ~~Further analyses indicate that the asymmetric OMZs in the tropical Pacific are attributable to the asymmetry in both physical supply and. On the other hand, applying a reduced O:C utilization ratio leads to a large decrease in biological consumption. The larger volume of northern OMZ is a result of greater biological consumption, and weaker a small decrease in physical supply (due to the north, in which vertical changes in DO gradients). These findings point to strong physical supply plays a dominant role in the lower OMZs but biological consumption also has impacts on the asymmetric DO for the upper OMZs.~~

495 ~~Future studies utilizing advanced models are needed to better understand the impacts of physical and biological interactions on the variability and drivers of feedbacks in the tropical Pacific OMZs.~~

~~*Code and data availability.* The exact version of the software code used to produce the results presented in this paper is archived on Zenodo (<http://doi.org/10.5281/zenodo.4384131>, Wang et al., 2020). Other code and data are available upon request from the authors. Request for materials should be addressed to X.J.W. (xwang@bnu.edu.cn).~~

~~*Author contributions.* X.J.W. and K.W. designed the study, performed the simulations and prepared the manuscript. R.M., D.X.Z. and R.H.Z. contributed to analysis, interpretation of results and writing.~~

~~*Competing interests.* The authors declare that they have no conflict of interest.~~

~~*Acknowledgements.* This work was supported by the Chinese Academy of Sciences' Strategic Priority Project (XDA1101010504). The authors wish to acknowledge the use of the Ferret (<http://ferret.pmel.noaa.gov/Ferret/>).~~

## References

- Bao, Y., Li, Y., 2016. Simulations of dissolved oxygen concentration in CMIP5 Earth system models. *Acta Oceanologica Sinica* 35, 28–37.
- 515 Berthet, S., S  f  rian, R., Bricaud, C., Chevallier, M., Voldoire, A., Eth  , C., 2019. Evaluation of an Online Grid–Coarsening Algorithm in a Global Eddy – Admitting Ocean Biogeochemical Model. *Journal of Advances in Modeling Earth Systems* 11, 1759–1783.
- Bettencourt, J.H., Lopez, C., Hernandez-Garcia, E., Montes, I., Sudre, J., Dewitte, B., Paulmier, A., Garc  n, V., 2015. Boundaries of the Peruvian oxygen minimum zone shaped by coherent mesoscale dynamics. *Nature Geoscience* 8, 937–967.
- 520 Bopp, L., Le Qu  re, C., Heimann, M., Manning, A.C., Monfray, P., 2002. Climate-induced oceanic oxygen fluxes: Implications for the contemporary carbon budget. *Global Biogeochemical Cycles* 16, 1–13.
- Brandt, P., Bange, H.W., Banyte, D., Dengler, M., Didwischus, S.H., Fischer, T., Greatbatch, R.J., Hahn, J., Kanzow, T., Karstensen, J., Krortzinger, A., Krahnmann, G., Schmidtke, S., Stramma, L., Tanhua, T., Visbeck, M., 2015. On the role of circulation and mixing in the ventilation of oxygen minimum zones with a focus on the eastern tropical North Atlantic. *Biogeosciences* 12, 489–512.
- 525 Breitburg, D., Levin, L.A., Oschlies, A., Gregoire, M., Chavez, F.P., Conley, D.J., Garc  n, V., Gilbert, D., Gutierrez, D., Isensee, K., Jacinto, G.S., Limburg, K.E., Montes, I., Naqvi, S.W.A., Pitcher, G.C., Rabalais, N.N., Roman, M.R., Rose, K.A., Seibel, B.A., Telszewski, M., Yasuhara, M., Zhang, J., 2018. Declining oxygen in the global ocean and coastal waters. *Science* 359.
- 530 Brewer, P.G., Peltzer, E.T., 2016. Ocean chemistry, ocean warming, and emerging hypoxia: Commentary. *Journal of Geophysical Research: Oceans* 121, 3659–3667.
- Busecke, J.J.M., Resplandy, L., Dunne, J.P.P., 2019. The Equatorial Undercurrent and the Oxygen Minimum Zone in the Pacific. *Geophysical Research Letters*, 6716–6725.
- 535 Cabre, A., Marinov, I., Bernardello, R., Bianchi, D., 2015. Oxygen minimum zones in the tropical Pacific across CMIP5 models: mean state differences and climate change trends. *Biogeosciences* 12, 5429–5454.
- Cavan, E.L., Trimmer, M., Shelley, F., Sanders, R., 2017. Remineralization of particulate organic carbon in an ocean oxygen minimum zone. *Nature communications* 8, 14847.
- 540 Chen, D., Rothstein, L.M., Busalacchi, A.J., 1994. A Hybrid Vertical Mixing Scheme and Its Application to Tropical Ocean Models. *Journal of Physical Oceanography* 24, 2156–2179.
- Czeschel, R., Stramma, L., Johnson, G.C., 2012. Oxygen decreases and variability in the eastern equatorial Pacific. *J Geophys Res Oceans* 117, 1–12.
- 545 Czeschel, R., Stramma, L., Schwarzkopf, F.U., Giese, B.S., Funk, A., Karstensen, J., 2011. Middepth circulation of the eastern tropical South Pacific and its link to the oxygen minimum zone. *J Geophys Res Oceans* 116.
- Duteil, O., Oschlies, A., 2011. Sensitivity of simulated extent and future evolution of marine suboxia to mixing intensity. *Geophysical Research Letters* 38.
- 550 Feely, R.A., Sabine, C.L., Schlitzer, R., Bullister, J.L., Mecking, S., Greeley, D., 2004. Oxygen utilization and organic carbon remineralization in the upper water column of the Pacific Ocean. *Journal of Oceanography* 60, 45–52.
- Fiedler, P.C., Talley, L.D., 2006. Hydrography of the eastern tropical Pacific: A review. *Progress in Oceanography* 69, 143–180.
- 555 Fu, W.W., Bardin, A., Primeau, F., 2018. Tracing ventilation source of tropical Pacific oxygen minimum zones with an adjoint global ocean transport model. *Deep Sea Research Part I: Oceanographic Research Papers* 139, 95–103.
- Garc  n, V., Karstensen, J., Palacz, A., Telszewski, M., Aparicio-Lara, T., Breitburg, D., Chavez, F., Coelho, P., Cornejo-D’Ottone, M., Santos, C., Fiedler, B., Gallo, N.D., Gr  goire, M., Gutierrez, D., Hernandez-Ayon, M., Isensee, K., Koslow, T., Levin, L., Marsac, F., Maske, H., Mbaye, B.C., Montes, I., Naqvi, W., Pearlman, J., Pinto, E., Pitcher, G., Pizarro, O., Rose, K., Shenoy, D., Van der Plas, A., Vito, M.R., Weng, K., 2019. Multidisciplinary Observing in the World Ocean’s Oxygen Minimum Zone Regions: From Climate to Fish — The VOICE Initiative. *Frontiers in Marine Science* 6.
- Gnanadesikan, A., Bianchi, D., Pradal, M.A., 2013. Critical role for mesoscale eddy diffusion in supplying oxygen to hypoxic ocean waters. *Geophysical Research Letters* 40, 5194–5198.

- 560 Kalnay, E., Kanamitsu, M., Kistler, R., Collins, W., Deaven, D., Gandin, L., Iredell, M., Saha, S., White, G., Woollen, J.,  
Zhu, Y., Chelliah, M., Ebisuzaki, W., Higgins, W., Janowiak, J., Mo, K.C., Ropelewski, C., Wang, J., Leetmaa, A.,  
Reynolds, R., Jenne, R., Joseph, D., 1996. The NCEP/NCAR 40-year reanalysis project. *B Am Meteorol Soc* 77, 437–471.
- 565 Kalvelage, T., Lavik, G., Jensen, M.M., Revsbech, N.P., Løsecher, C., Schunck, H., Desai, D.K., Hauss, H., Kiko, R.,  
Holtappels, M., LaRoche, J., Schmitz, R.A., Graco, M.I., Kuypers, M.M., 2015. Aerobic microbial respiration in oceanic  
oxygen minimum zones. *PLoS one* 10.
- Karstensen, J., Stramma, L., Visbeck, M., 2008. Oxygen minimum zones in the eastern tropical Atlantic and Pacific oceans.  
*Progress in Oceanography* 77, 331–350.
- Keller, D.P., Kriest, I., Koeve, W., Oeschlies, A., 2016. Southern Ocean biological impacts on global ocean oxygen.  
*Geophysical Research Letters* 43, 6469–6477.
- 570 Kessler, W.S., 2006. The circulation of the eastern tropical Pacific: A review. *Progress in Oceanography* 69, 181–217.
- Kug, J.S., Kang, I.S., An, S.I., 2003. Symmetric and antisymmetric mass exchanges between the equatorial and off-  
equatorial Pacific associated with ENSO. *Journal of Geophysical Research: Oceans* 108.
- Kuntz, L.B., Schrag, D.P., 2018. Hemispheric asymmetry in the ventilated thermocline of the Tropical Pacific. *Journal of  
Climate* 31, 1281–1288.
- 575 Levin, L.A., 2018. Manifestation, Drivers, and Emergence of Open-Ocean Deoxygenation. *Annual review of marine science*  
10, 229–260.
- Libby, P.S., Wheeler, P.A., 1997. Particulate and dissolved organic nitrogen in the central and eastern equatorial Pacific.  
*Deep Sea Research Part I: Oceanographic Research Papers* 44, 345–361.
- 580 Llanillo, P.J., Pelegri, J.L., Talley, L.D., Pena-Izquierdo, J., Cordero, R.R., 2018. Oxygen Pathways and Budget for the  
Eastern South Pacific Oxygen Minimum Zone. *Journal of Geophysical Research: Oceans* 123, 1722–1744.
- Loginova, A.N., Thomsen, S., Dengler, M., Ludke, J., Engel, A., 2019. Diapycnal dissolved organic matter supply into the  
upper Peruvian oxycline. *Biogeosciences* 16, 2033–2047.
- Murtugudde, R., Seager, R., Busalacchi, A., 1996. Simulation of the tropical oceans with an ocean GCM coupled to an  
atmospheric mixed-layer model. *Journal of Climate* 9, 1795–1815.
- 585 Oeschlies, A., Brandt, P., Stramma, L., Schmidtko, S., 2018. Drivers and mechanisms of ocean deoxygenation. *Nature  
Geoscience* 11, 467–473.
- Paulmier, A., Ruiz-Pino, D., 2009. Oxygen minimum zones (OMZs) in the modern ocean. *Progress in Oceanography* 80,  
113–128.
- Raimbault, P., Slawyk, G., Boudjellal, B., Coatanoan, C., Conan, P., Coste, B., Garcia, N., Moutin, T., Pujol-Pay, M., 1999.  
590 Carbon and nitrogen uptake and export in the equatorial Pacific at 150°W: Evidence of an efficient regenerated production  
cycle. *Journal of Geophysical Research: Oceans* 104, 3341–3356.
- Schmidtko, S., Stramma, L., Visbeck, M., 2017. Decline in global oceanic oxygen content during the past five decades.  
*Nature* 542, 335–339.
- 595 Shigemitsu, M., Yamamoto, A., Oka, A., Yamanaka, Y., 2017. One possible uncertainty in CMIP5 projections of low-  
oxygen water volume in the Eastern Tropical Pacific. *Geophysical Research Letters* 31, 804–820.
- Sonnerup, R.E., Mecking, S., Bullister, J.L., 2013. Transit time distributions and oxygen utilization rates in the Northeast  
Pacific Ocean from chlorofluorocarbons and sulfur hexafluoride. *Deep Sea Res Pt I* 72, 61–71.
- Stramma, L., Johnson, G.C., Firing, E., Schmidtko, S., 2010. Eastern Pacific oxygen minimum zones: Supply paths and  
multidecadal changes. *J Geophys Res Oceans* 115.
- 600 Stramma, L., Johnson, G.C., Sprintall, J., Mohrholz, V., 2008. Expanding oxygen minimum zones in the tropical oceans.  
*Science* 320, 655–658.
- Stramma, L., Oeschlies, A., Schmidtko, S., 2012. Mismatch between observed and modeled trends in dissolved upper-ocean  
oxygen over the last 50 yr. *Biogeosciences* 9, 4045–4057.
- 605 Talley, L.D., Feely, R.A., Sloyan, B.M., Wanninkhof, R., Baringer, M.O., Bullister, J.L., Carlson, C.A., Doney, S.C., Fine,  
R.A., Firing, E., Gruber, N., Hansell, D.A., Ishii, M., Johnson, G.C., Katsumata, K., Key, R.M., Kramp, M., Langdon, C.,  
Macdonald, A.M., Mathis, J.T., McDonagh, E.L., Mecking, S., Millero, F.J., Mordy, C.W., Nakano, T., Sabine, C.L.,  
Smethie, W.M., Swift, J.H., Tanhua, T., Thurnherr, A.M., Warner, M.J., Zhang, J.Z., 2016. Changes in ocean heat, carbon  
content, and ventilation: a review of the first decade of global repeat hydrography. *Annual review of marine science*  
8, 185–215.

- 610 Tiano, L., Garcia Robledo, E., Dalsgaard, T., Devol, A.H., Ward, B.B., Ulloa, O., Canfield, D.E., Revsbech, N.P., 2014. Oxygen distribution and aerobic respiration in the north and south eastern tropical Pacific oxygen minimum zones. *Deep-Sea Research Part I: Oceanographic Research Papers* 94, 173–183.
- 615 Wang, X.J., Behrenfeld, M., Le Borgne, R., Murtugudde, R., Boss, E., 2009a. Regulation of phytoplankton carbon to chlorophyll ratio by light, nutrients and temperature in the Equatorial Pacific Ocean: a basin-scale model. *Biogeosciences* 6, 391–404.
- Wang, X.J., Le Borgne, R., Murtugudde, R., Busalacchi, A.J., Behrenfeld, M., 2008. Spatial and temporal variations in dissolved and particulate organic nitrogen in the equatorial Pacific: biological and physical influences. *Biogeosciences* 5, 1705–1721.
- 620 Wang, X.J., Murtugudde, R., Hackert, E., Wang, J., Beauchamp, J., 2015. Seasonal to decadal variations of sea surface pCO<sub>2</sub> and sea-air CO<sub>2</sub> flux in the equatorial oceans over 1984–2013: A basin-scale comparison of the Pacific and Atlantic Oceans. *Global Biogeochemical Cycles* 29, 597–609.
- Wang, X.J., Murtugudde, R., Le Borgne, R., 2009b. Nitrogen uptake and regeneration pathways in the equatorial Pacific: a basin-scale modeling study. *Biogeosciences* 6, 2647–2660.
- 625 Wanninkhof, R., 1992. Relationship between wind speed and gas exchange over the Ocean. *J Geophys Res-Oceans* 97, 7373–7382.
- Ward, B.A., Wilson, J.D., Death, R.M., Monteiro, F.M., Yool, A., Ridgwell, A., 2018. EcoGENIE 1.0: plankton ecology in the cGENIE Earth system model. *Geoscientific Model Development* 11, 4241–4267.
- Weiss, R.F., 1970. The solubility of nitrogen, oxygen and argon in water and seawater. *Deep-Sea Research* 17, 721–735.
- 630 Williams, J.H.T., Totterdell, I.J., Halloran, P.R., Valdes, P.J., 2014. Numerical simulations of oceanic oxygen cycling in the FAMOUS Earth System model: FAMOUS-ES, version 1.0. *Geoscientific Model Development* 7, 1419–1431.

## Tables

**Table 1.** Model experiments with different values for remineralization rate ( $C_{DON}$ ) and vertical background diffusion ( $K_b$ ).

Parameter	Unit	Reference	$C_{d0.5}$	$C_{d0.5}$ $K_{b0.1}$	$C_{d0.5}$ $K_{b0.3}$	$C_{d0.5}$ $K_{b0.5}$
$C_{DON}(0-100\text{ m})$	$d^{-1}$	0.001			0.0005	
$C_{DON}(100-600\text{ m})$		0.001-0.0005			0.0005-0.00025	
$C_{DON}(600-1000\text{ m})$		0.0005			0.00025	
$K_b$	$cm^2 s^{-1}$	0	0	0.1	0.3	0.5

635

**Table 2.** Statistics for DO ( $mmol\ m^{-3}$ ) comparisons between WOA2013 and model experiments over 1981-2000 in the Eastern Tropical North Pacific (ETNP) and Eastern Tropical South Pacific (ETSP).

Layers	Statistics	ETNP (165°W-90°W, 5°N-20°N)					ETSP (110°W-80°W, 10°S-3°S)				
		Reference	$C_{d0.5}$	$C_{d0.5}$ $K_{b0.1}$	$C_{d0.5}$ $K_{b0.3}$	$C_{d0.5}$ $K_{b0.5}$	Reference	$C_{d0.5}$	$C_{d0.5}$ $K_{b0.1}$	$C_{d0.5}$ $K_{b0.3}$	$C_{d0.5}$ $K_{b0.5}$
200-400 (m)	Bias	-9.45	-4.00	-3.96	-3.82	-3.60	-11.89	-3.59	-3.33	-2.67	-1.84
	MAE	15.17	15.70	15.56	15.27	14.98	11.89	3.72	3.55	3.15	3.12
	RMSE	19.01	17.34	17.18	16.82	16.44	12.18	4.44	4.28	3.92	3.57
400-700 (m)	Bias	-7.24	-4.99	-4.19	-2.49	-0.72	-10.36	-7.17	-5.79	-2.92	-0.04
	MAE	9.01	8.25	7.99	7.44	6.95	10.38	7.99	7.12	5.59	4.85
	RMSE	10.86	9.72	9.29	8.48	7.88	12.33	9.61	8.54	6.75	5.88
700-1000 (m)	Bias	-7.19	-4.49	-2.44	1.08	3.98	-12.90	-9.11	-6.48	-2.34	0.78
	MAE	7.18	4.67	4.12	4.17	5.28	13.33	10.42	8.81	6.98	6.47
	RMSE	9.22	6.85	5.49	4.67	5.92	16.14	12.81	10.79	8.33	7.59

640

**Table 3.** Comparisons of OMZ volume ( $10^{15}\ m^3$ ) between WOA2013 and sensitivity experiments.

Regions	Waters	WOA2013	Reference	$C_{d0.5}$	$C_{d0.5}$ $K_{b0.1}$	$C_{d0.5}$ $K_{b0.3}$	$C_{d0.5}$ $K_{b0.5}$
North Pacific	Suboxic	5.97	10.47	8.87	8.29	7.36	6.61
	Hypoxic	19.98	21.21	20.48	20.35	20.01	19.62
South Pacific	Suboxic	1.43	3.49	2.42	2.20	1.85	1.56
	Hypoxic	7.12	9.90	8.73	8.35	7.70	7.13

Suboxic:  $DO < 20\ mmol\ m^{-3}$ ; Hypoxic:  $DO < 60\ mmol\ m^{-3}$ .

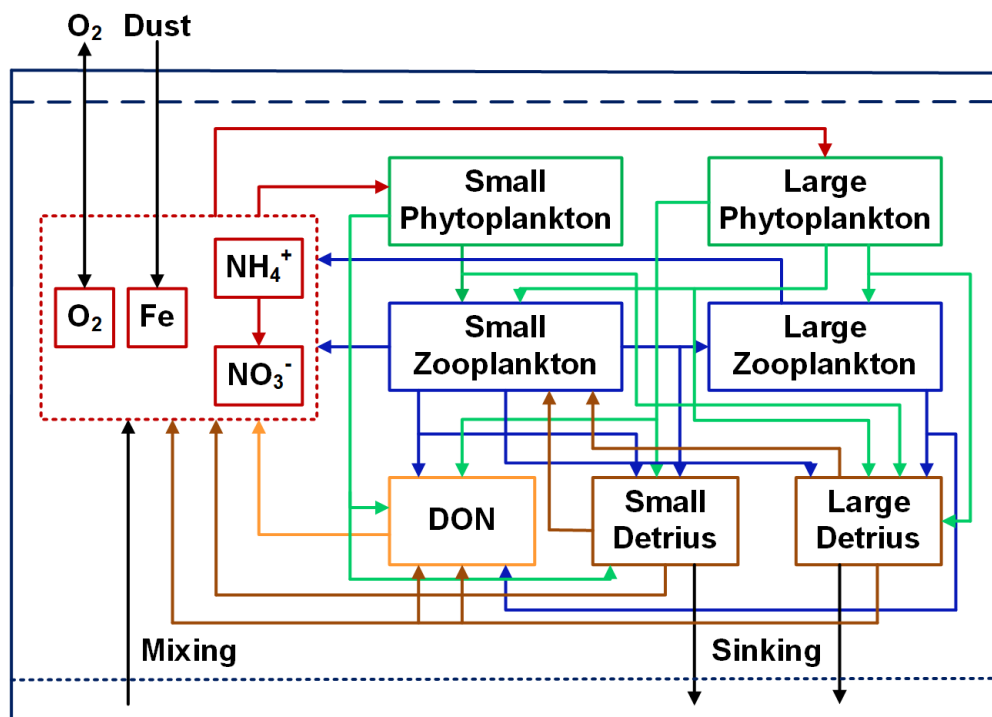


**Figure 1.** Flow diagram of ecosystem model. Red, green, blue, yellow and brown lines and arrows denote fluxes originating from inorganic forms, phytoplankton, zooplankton, DON and detritus, respectively.



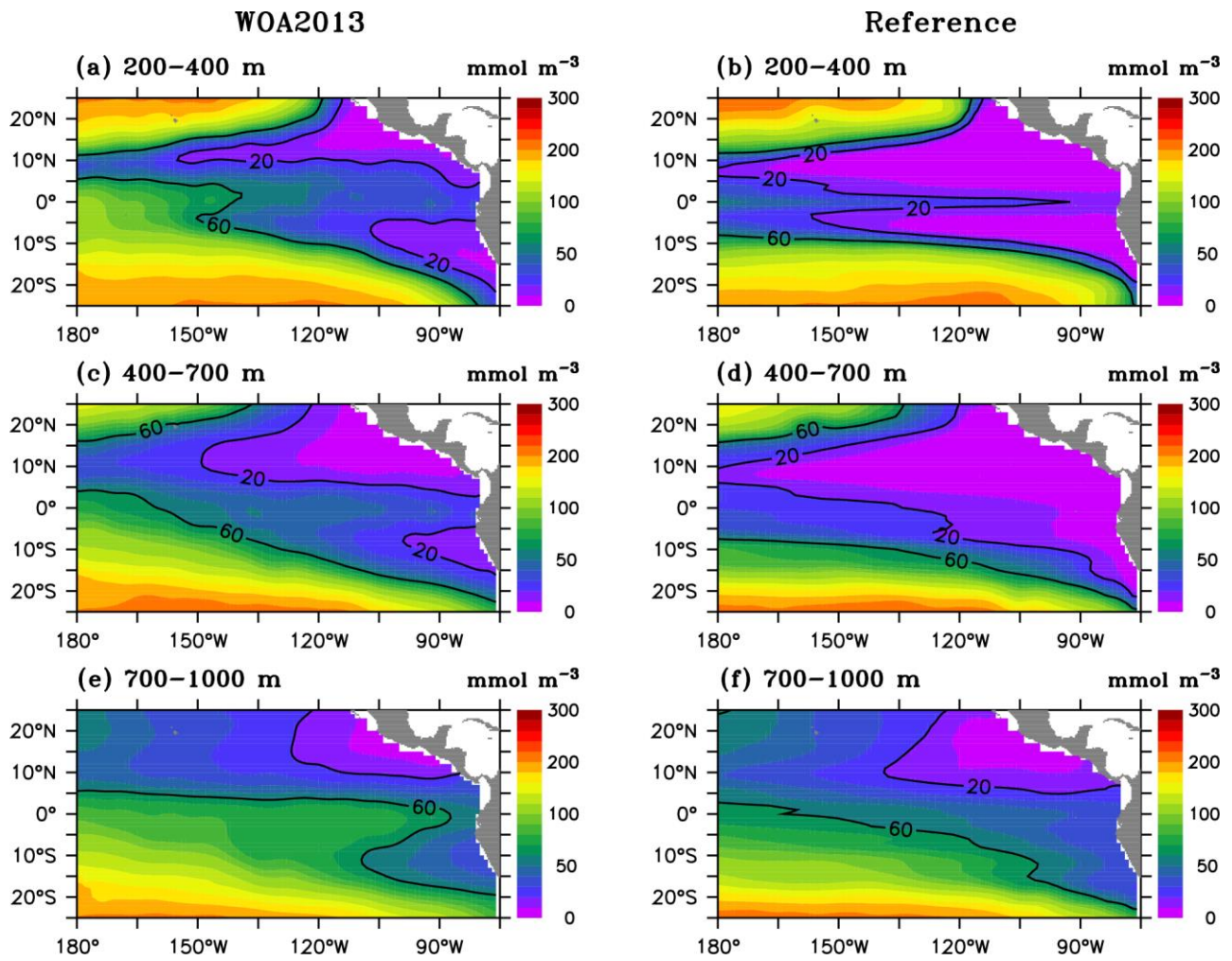


**Figure 2.** Comparisons of DO concentration between WOA2013 (left panel) and reference run during 1981-2000 (right panel).

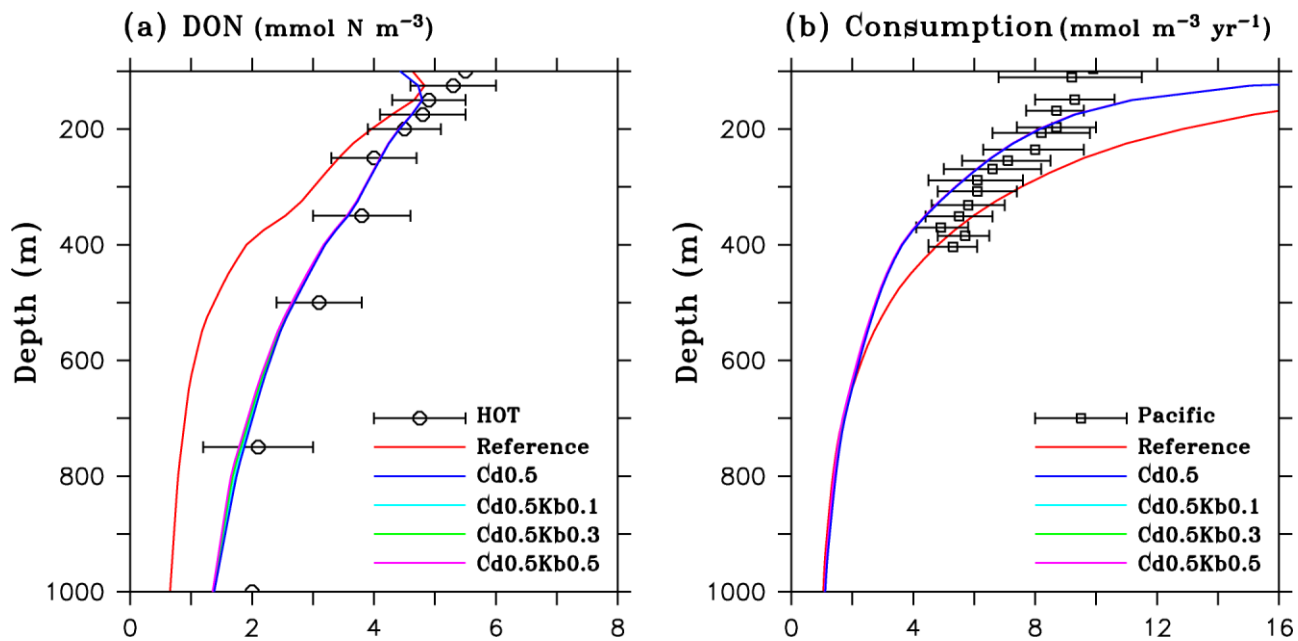
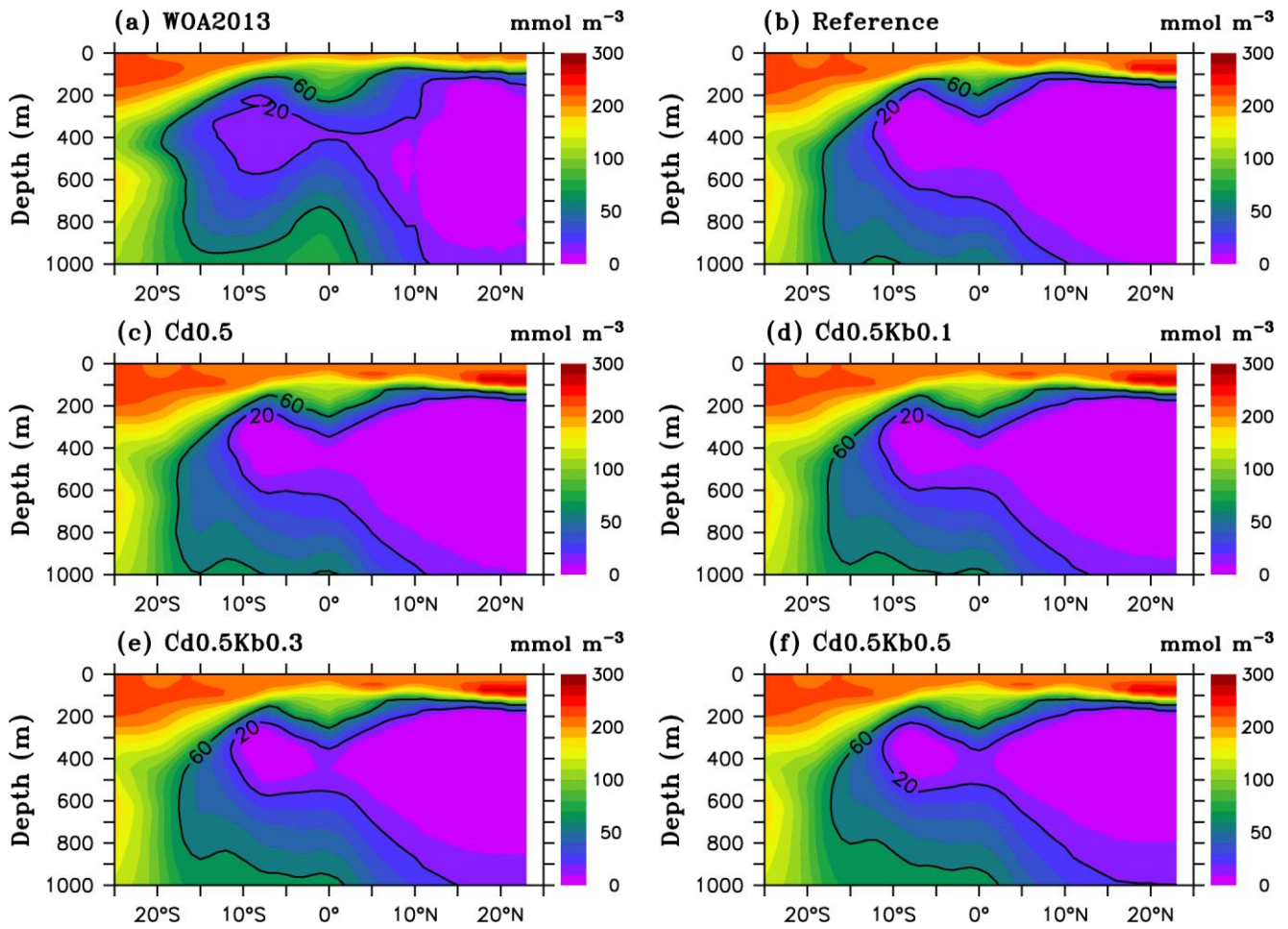


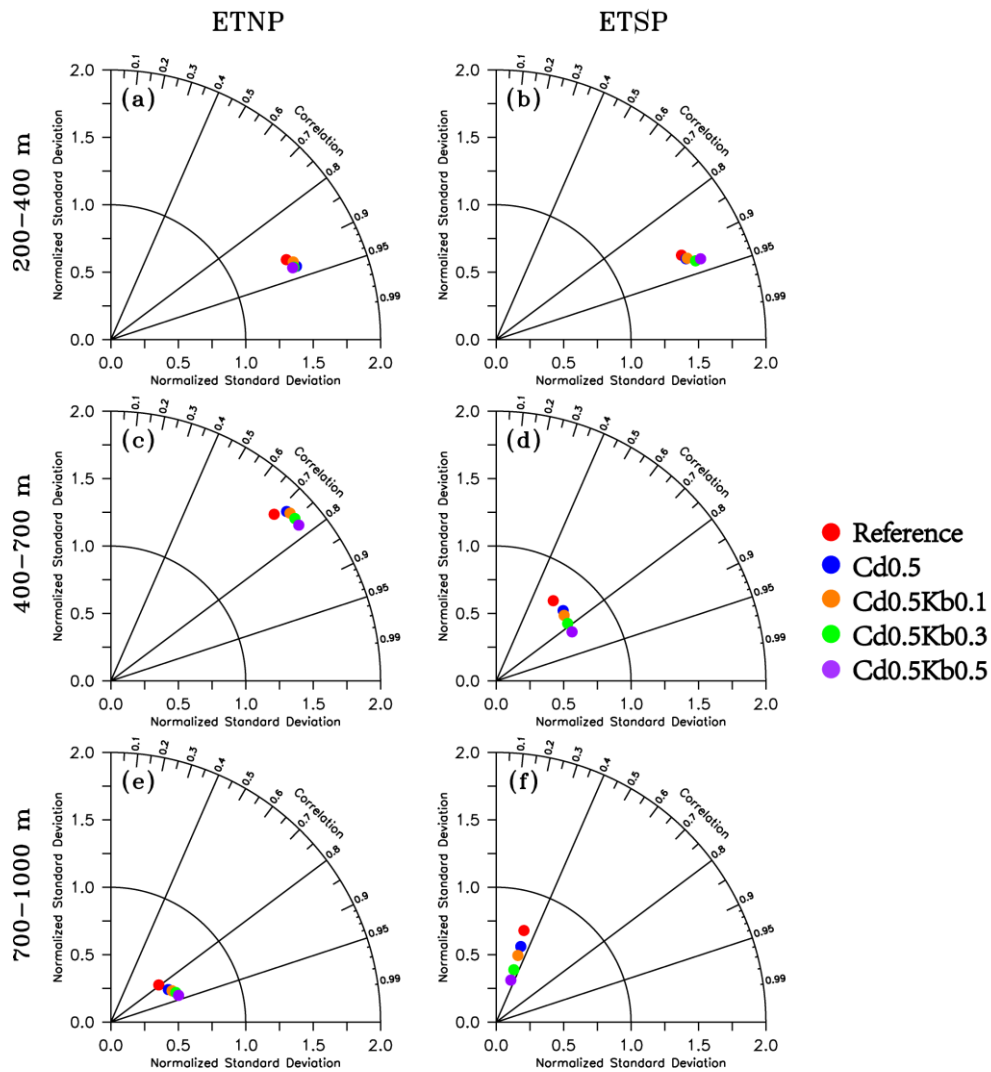
**Figure 3.** Comparisons of DON concentration (a) and consumption rate (b) between observation and model experiments. Observed DON data are from Hawaii Ocean Time-series program (HOT, 22°45'N, 158°00'W) ([https://hahana.soest.hawaii.edu/hot/hot\\_jgofs.html](https://hahana.soest.hawaii.edu/hot/hot_jgofs.html)). Observed consumption data are obtained from Karastensen et al., (2008) for the entire Pacific.

660



665

**Figure 4.** Observed and simulated DO from model experiments over  $110^{\circ}\text{W}$ – $85^{\circ}\text{W}$ . (a) WOA2013, (b) reference run, (c) Cd0.5, (d) Cd0.5Kb0.1, (e) Cd0.5Kb0.3, and (f) Cd0.5Kb0.5 over 1981–2000.



670 **Figure 5.** Taylor diagrams performed on the simulation of DO concentration between WOA2013 and model experiments for the left panel (ETNP: 165°W 90°W, 5°N 20°N) and right panel (ETSP: 110°W 80°W, 10°S 3°S) over 200-400 m, 400-700 m, and 700-1000 m.

Cruise data

Model (Cd0.5Kb0.5)

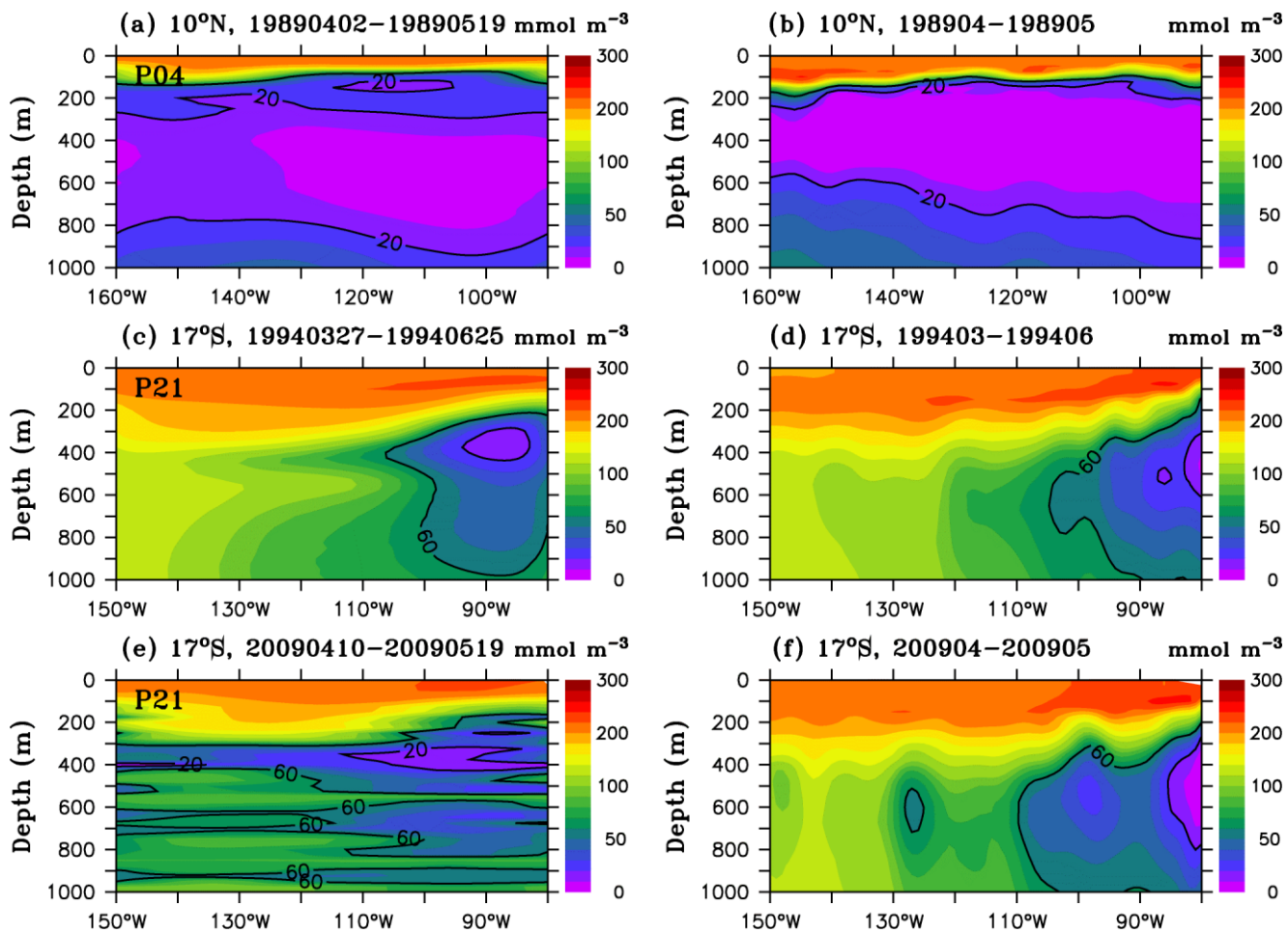


**Figure 6.** Distribution of DO from cruise data (left panel) and model results (right panel). Observed DO along the P04 and P21 lines are from CCHDO (<https://echdo.ucsd.edu/>), which provides access to high quality global CTD and hydrographic data from GO-SHIP, WOCE, CLIVAR and other repeat hydrography programs.

675

680



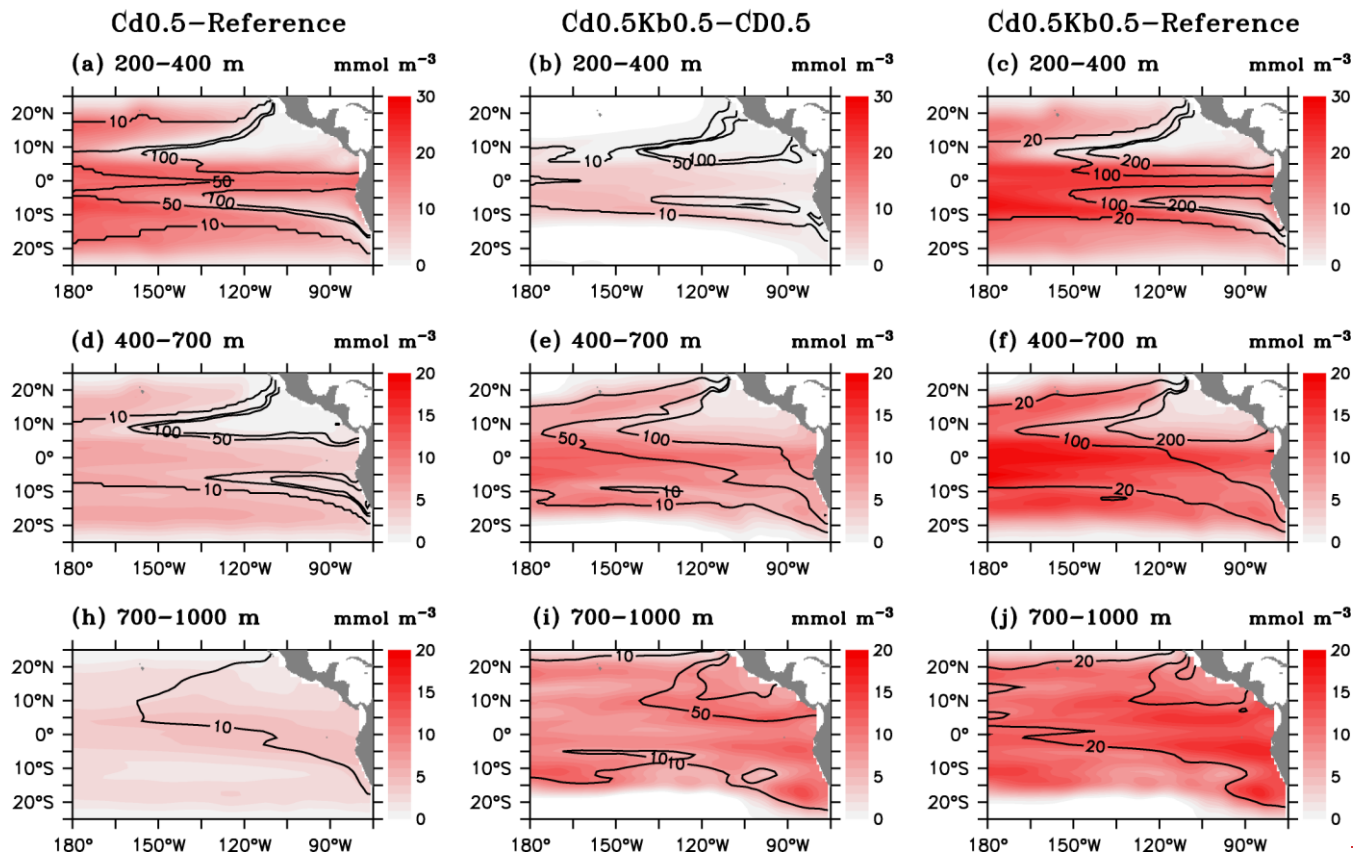
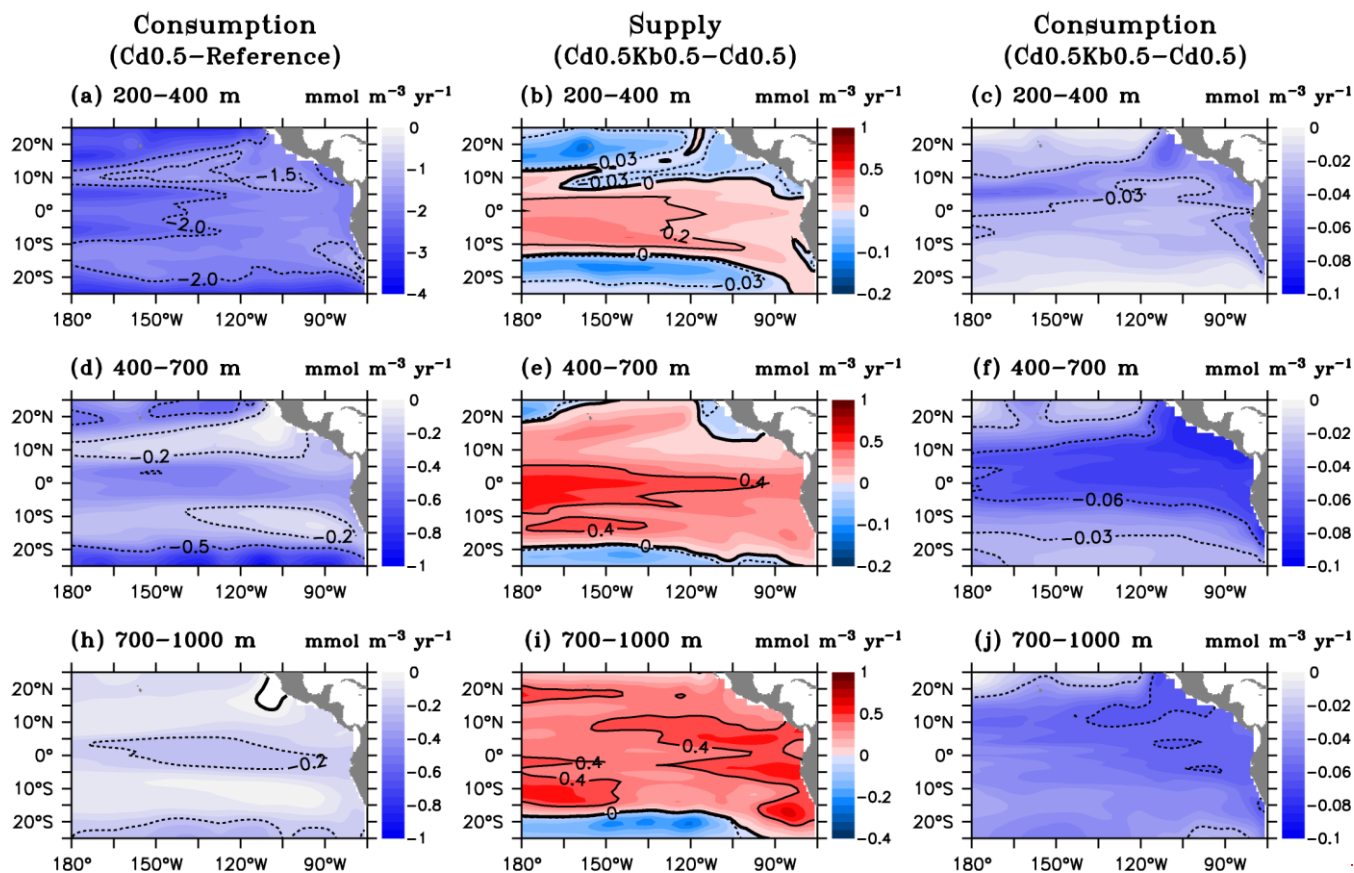


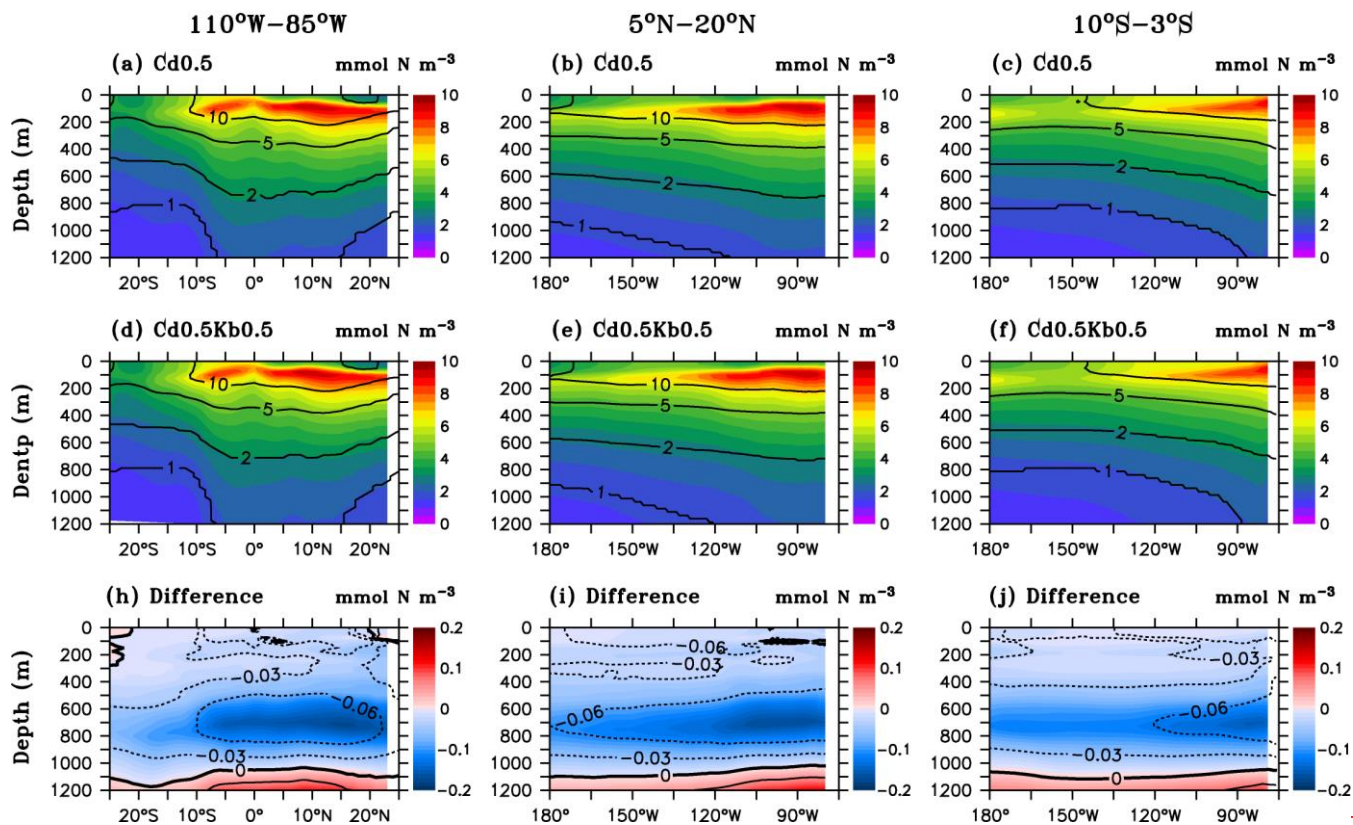
**Figure 7.** Changes of DO concentration due to reduced remineralization rate (left panel, Cd0.5 minus reference), enhanced mixing (middle panel, Cd0.5Kb0.5 minus Cd0.5), and their combination (right panel, Cd0.5Kb0.5 minus reference).

685 Superimposed solid black lines denote the percentage of DO change relative to the reference run contoured by 10%, 50% and 100% in the left and middle panel, and 20%, 100% and 200% in the right panel.



690 **Figure 8.** Decrease of DO consumption due to reduced remineralization rate (left panel, Cd0.5 minus reference), and changes in DO supply (middle panel, Cd0.5Kb0.5 minus Cd0.5) and decrease of DO consumption due to enhanced mixing (right panel, Cd0.5Kb0.5 minus Cd0.5).

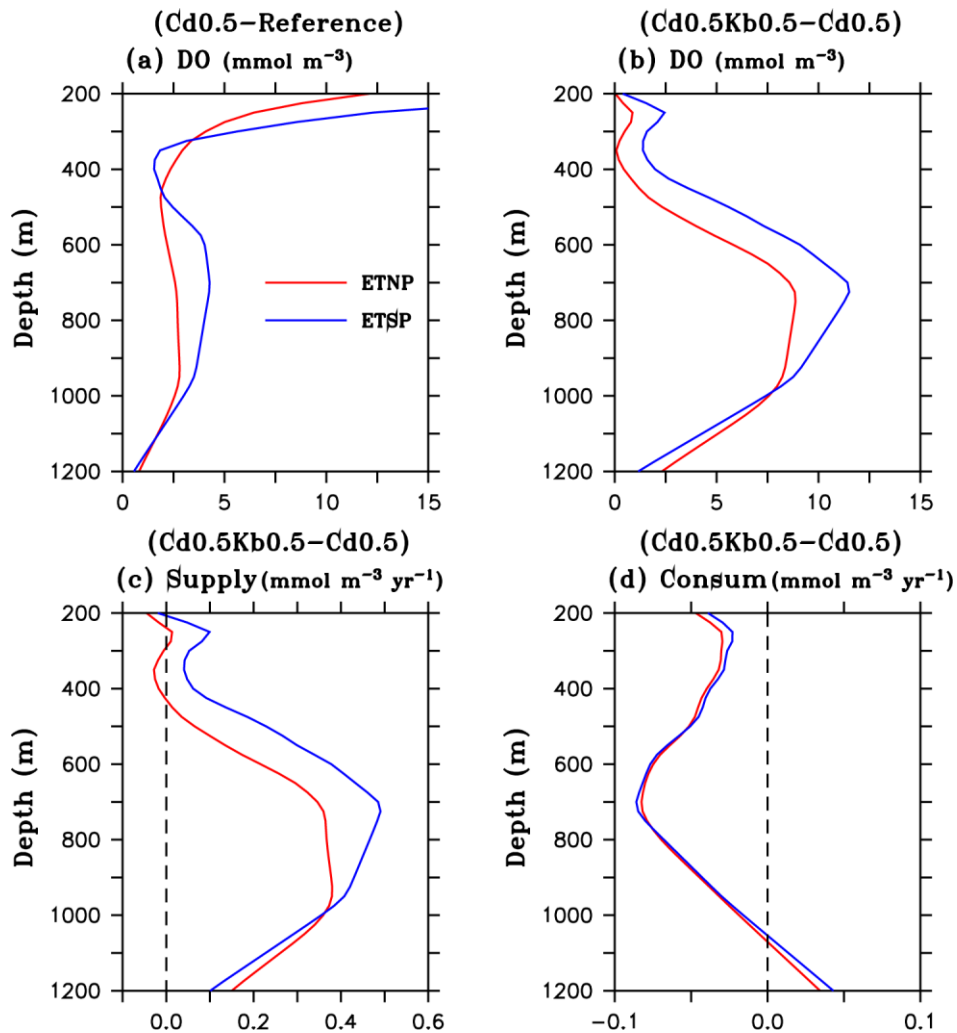




695

**Figure 9.** Distribution of DON and DON remineralization ( $\text{mmol m}^{-3}\text{-yr}^{-1}$ ) over  $110^{\circ}\text{W}$ – $85^{\circ}\text{W}$  (left panel),  $5^{\circ}\text{N}$ – $20^{\circ}\text{N}$  (middle panel), and  $10^{\circ}\text{S}$ – $3^{\circ}\text{S}$  (right panel) from (a–e) Cd0.5, (d–f) Cd0.5Kb0.5, and (g–i) their differences (Cd0.5Kb0.5 minus Cd0.5). Superimposed black lines denote consumption rate ( $\text{mmol m}^{-3}\text{-yr}^{-1}$ ) by remineralization of DON in (a–f) and the difference of consumption rate between Cd0.5Kb0.5 and Cd0.5 in (g–i).

700



705

**Figure 10.** Changes due to reduced remineralization rate (Cd0.5 minus reference) for (a) DO, and enhanced mixing (Cd0.5Kb0.5 minus Cd0.5) for (b) DO, (c) physical supply, and (d) biological consumption. ETNP: 165°W–90°W, 5°N–20°N; ETSP: 110°W–80°W, 10°S–3°S.

710

This study suggest that biological consumption (i.e., greater rate to the south) cannot explain the asymmetric feature in the tropical Pacific OMZs (i.e., lower DO levels to the north), but physical processes (i.e., stronger supply to the south) play a major role in shaping the asymmetric OMZs of the tropical Pacific. In addition, the interactions between physical and biological processes are also stronger in the southern OMZ than in the northern OMZ, probably because physical supply is sensitive to changes in both parameterizations of vertical mixing and DOM remineralization. Further studies with improved approaches will enable to better understand the interactions and feedbacks between physical and biogeochemical processes.

715

## Appendix A

### Model biogeochemical equations

720

#### Phytoplankton equations

$$\frac{\partial P_S}{\partial t} = \mu_S P_S - g_{P_S}(1 - e^{-\Lambda P_S}) Z_S - m_S P_S \quad (\text{B1})$$

$$\frac{\partial P_L}{\partial t} = \mu_L P_L - g_{P_{L1}}(1 - e^{-\Lambda P_L}) Z_L - g_{P_{L2}}(1 - e^{-\Lambda P_L}) Z_S - m_L P_L \quad (\text{B2})$$

#### 725 Zooplankton equations

$$\frac{\partial Z_S}{\partial t} = [\lambda(g_{P_S}(1 - e^{-\Lambda P_S}) + g_{P_{L2}}(1 - e^{-\Lambda P_L})) + g_{D_S}(1 - e^{-\Lambda D_S}) + g_{D_{L2}}(1 - e^{-\Lambda D_L}) - (r_S + \delta_S)] Z_S - g_{Z_S}(1 - e^{-\Lambda Z_S}) Z_L \quad (\text{B3})$$

$$\frac{\partial Z_L}{\partial t} = [\lambda(g_{P_{L1}}(1 - e^{-\Lambda P_L}) + g_{Z_S}(1 - e^{-\Lambda Z_S})) + g_{D_{L1}}(1 - e^{-\Lambda D_L}) - (r_L + \delta_L)] Z_L \quad (\text{B4})$$

#### 730 Detritus equations

$$\frac{\partial D_S}{\partial t} = (m_S P_S + m_L P_L + (r_S Z_S + r_L Z_L) \chi)(1 - \gamma) - g_{D_S}(1 - e^{-\Lambda D_S}) Z_S - (c_{D_S} + \omega_{D_S} h^{-1}) D_S \quad (\text{B5})$$

$$\frac{\partial D_L}{\partial t} = (1 - \lambda) [(g_{P_S}(1 - e^{-\Lambda P_S}) + g_{P_{L2}}(1 - e^{-\Lambda P_L})) Z_S + (g_{P_{L1}}(1 - e^{-\Lambda P_L}) + g_{Z_S}(1 - e^{-\Lambda Z_S})) Z_L] + \delta_S Z_S + \delta_L Z_L - (c_{D_L} + \omega_{D_L} h^{-1}) D_L - g_{D_{L2}}(1 - e^{-\Lambda D_L}) Z_S - g_{D_{L1}}(1 - e^{-\Lambda D_L}) Z_L \quad (\text{B6})$$

#### 735 DON equations

$$\frac{\partial DON}{\partial t} = (m_S P_S + m_L P_L + (r_S Z_S + r_L Z_L) \chi) \gamma + (c_{D_S} D_S + c_{D_L} D_L) \zeta - c_{DON} DON \quad (\text{B7})$$

#### Nutrients equations

$$\frac{\partial \text{NO}_3}{\partial t} = -\mu_S P_S \frac{N_{S_{UP}}}{N_{S_{UP}+A_{UP}}} - \mu_L P_L \frac{N_{L_{UP}}}{N_{L_{UP}+A_{UP}}} + \varphi \text{NH}_4 \quad (\text{B8})$$

$$740 \quad \frac{\partial \text{NH}_4}{\partial t} = -\mu_S P_S \frac{A_{up}}{N_{S_{UP}+A_{UP}}} - \mu_L P_L \frac{A_{up}}{N_{L_{UP}+A_{UP}}} + (r_S Z_S + r_L Z_L)(1 - \chi) + c_{DON} DON + (c_{D_S} D_S + c_{D_L} D_L)(1 - \zeta) - \varphi \text{NH}_4 \quad (\text{B9})$$

$$\frac{\partial \text{Fe}}{\partial t} = -(\mu_S P_S R_S + \mu_L P_L R_L - s_{Fe} D_L F_e) + R_S [(r_S Z_S + r_L Z_L)(1 - \chi) + c_{DON} DON + c_{D_S} D_S + c_{D_L} D_L (1 - \zeta)] \quad (\text{B10})$$

#### Nitrogen uptake

$$745 \quad N_{S\_UP} = \frac{NO_3}{K_{S\_NO_3} + NO_3} \left(1 - \frac{NH_4}{K_{NH_4} + NH_4}\right) \quad (B11)$$

$$N_{L\_UP} = \frac{NO_3}{K_{L\_NO_3} + NO_3} \left(1 - \frac{NH_4}{K_{NH_4} + NH_4}\right) \quad (B12)$$

$$A_{UP} = \frac{NH_4}{K_{NH_4} + NH_4} \quad (B13)$$

### Other equations

750

#### Phytoplankton growth rate

$$\mu_S = \mu_{S0} e^{k_T T} f(I) \psi_S(N, Fe) \quad (B14)$$

$$\mu_L = \mu_{L0} e^{k_T T} f(I) \psi_L(N, Fe) \quad (B15)$$

#### 755 Nutrient limitation

$$\psi_S(N, Fe) = \min\left(\frac{NO_3 + NH_4}{K_{S\_N} + NO_3 + NH_4}, \frac{Fe}{K_{S\_Fe} + Fe}\right) \quad (B16)$$

$$\psi_L(N, Fe) = \min\left(\frac{NO_3 + NH_4}{K_{L\_N} + NO_3 + NH_4}, \frac{Fe}{K_{L\_Fe} + Fe}\right) \quad (B17)$$

#### Light limitation

$$760 \quad f(I) = 1 - e^{-\frac{\alpha I}{\eta P_{MAX}}} \quad (B18)$$

#### Light attenuation

$$I(z) = I_0 \exp^{-k_A z} \quad (B19)$$

$$k_A = k_W + k_C \text{Chl} + k_D (D_S + D_L) \quad (B20)$$

765

#### Detritus decomposition and DON remineralization

$$c_{DS} = c_{DS0} e^{\frac{k_B(T-10)}{10}} e^{k_B(T-T_0)} \quad (B21)$$

$$770 \quad c_{DL} = c_{DL0} e^{\frac{k_B(T-10)}{10}} e^{k_B(T-T_0)} \quad (B22)$$

$$c_{DON} = c_{DON0} e^{\frac{k_B(T-10)}{10}} e^{k_B(T-T_0)} \quad (B23)$$

#### Phytoplankton carbon to chlorophyll ratio ( $\eta$ )

$$775 \quad \text{Chl} = \left( \frac{P_S}{\eta_S} + \frac{P_L}{\eta_L} \right) R_{C:N} \quad \text{-(B24)}$$

$$\eta_S = \eta_{S0} - (\eta_{S0} - \eta_{MIN}) \frac{\ln I_0 - \ln I}{4.605} \quad \text{-(B25)}$$

$$\eta_L = \eta_{L0} - (\eta_{L0} - \eta_{MIN}) \frac{\ln I_0 - \ln I}{4.605} \quad \text{-(B26)}$$

$$\eta_{S0} = \eta_{S\_MAX} - k_{PS} \mu_S^* \quad \text{-(B27)}$$

$$\eta_{L0} = \eta_{L\_MAX} - k_{PL} \mu_L^* \quad \text{-(B28)}$$

$$780 \quad \mu_S^* = \mu_{S0} e^{k_T T} \min \left( \frac{NO_3}{K_{S\_N} + NO_3}, \frac{Fe}{K_{S\_Fe} + Fe} \right) \quad \text{-(B29)}$$

$$\mu_L^* = \mu_{L0} e^{k_T T} \min \left( \frac{NO_3}{K_{L\_N} + NO_3}, \frac{Fe}{K_{L\_Fe} + Fe} \right) \quad \text{-(B30)}$$

## Appendix B

### 785 **Model biogeochemical parameters**

Symbol	Parameter	Unit	Value
$m_S$	Small phytoplankton mortality rate	$d^{-1}$	0.15
$m_L$	Large phytoplankton mortality rate	$d^{-1}$	0.35
$r_S$	Small zooplankton excretion rate	$d^{-1}$	0.53
$r_L$	Large zooplankton excretion rate	$d^{-1}$	0.44
$\delta_S$	Small zooplankton mortality rate	$d^{-1}$	0.12
$\delta_L$	Large zooplankton mortality rate	$d^{-1}$	0.12
$g_{PS}$	Maximum grazing rate for small phytoplankton	$d^{-1}$	2.6
$g_{PL1}$	Maximum grazing rate for large phytoplankton	$d^{-1}$	1.2
$g_{ZS}$	Maximum grazing rate for small zooplankton	$d^{-1}$	1.7
$g_{PL2}$	Maximum grazing rate for large phytoplankton	$d^{-1}$	0.9
$g_{DS}$	Maximum grazing rate for small detritus	$d^{-1}$	1.0
$g_{DL1}$	Maximum grazing rate for large detritus	$d^{-1}$	3.0
$g_{DL2}$	Maximum grazing rate for large detritus	$d^{-1}$	1.5
$\Lambda$	Ivlev coefficient	$(\text{mmol m}^{-3})^{-1}$	0.5
$\lambda$	Zooplankton assimilation coefficient	%	75
$\chi$	Excretion coefficient	%	55
$\gamma$	Dissolution coefficient	%	90
$\xi$	Dissolution coefficient	%	90
$R_{C:N}$	C:N ratio	mol:mol	6.625
$R_S$	Fe:N ratio for small phytoplankton	$\mu\text{mol:mol}$	15
$R_L$	Fe:N ratio for large phytoplankton	$\mu\text{mol:mol}$	40
$\eta_{S\_MIN}$	Minimum PhyC:Chl ratio in small phytoplankton	g:g	30
$\eta_{L\_MIN}$	Minimum PhyC:Chl ratio in large phytoplankton	g:g	15
$\eta_{S\_MAX}$	Maximum PhyC:Chl ratio in small phytoplankton	g:g	200
$\eta_{L\_MAX}$	Maximum PhyC:Chl ratio in large phytoplankton	g:g	120
$k_{PS}$	Photoacclimation coefficient for small phytoplankton	(g:g)d	95
$k_{PL}$	Photoacclimation coefficient for large phytoplankton	(g:g)d	70
$w_{DS}$	Sinking velocity for small detritus	$\text{m d}^{-1}$	1

$w_{DL}$	Sinking velocity for large detritus	$m d^{-1}$	3.5
$\phi$	Nitrification rate (when $I < 5 \mu mol E m^{-2} s^{-1}$ )	$d^{-1}$	0.04
$s_{Fe}$	Iron scavenge coefficient	$d^{-1} (nmol Fe m^{-3})^{-1}$	0.00001
$\mu_{S0}$	Maximum growth rate at $0^{\circ}C$ for small phytoplankton	$d^{-1}$	0.58
$\mu_{L0}$	Maximum growth rate at $0^{\circ}C$ for large phytoplankton	$d^{-1}$	1.16
$k_T$	Temp. Dependent coefficient for $\mu$	$^{\circ}C^{-1}$	0.06
$K_{S\_N}$	Half saturation constant for N limitation	$mmol m^{-3}$	0.3
$K_{L\_N}$	Half saturation constant for N limitation	$mmol m^{-3}$	0.9
$K_{S\_Fe}$	Half saturation constant for iron limitation	$mmol m^{-3}$	14
$K_{L\_Fe}$	Half saturation constant for iron limitation	$mmol m^{-3}$	150
$K_{S\_NO3}$	Half saturation constant for nitrate uptake	$mmol m^{-3}$	0.3
$K_{L\_NO3}$	Half saturation constant for nitrate uptake	$mmol m^{-3}$	0.9
$K_{NH4}$	Half saturation constant for ammonium uptake	$mmol m^{-3}$	0.05
$\alpha$	Initial slope of the P – I curve	$mg C mg chl^{-1} (\mu mol E m^{-2} s^{-1})^{-1}$	0.02
$P_{MAX}$	Maximum carbon specific growth rate	$h^{-1}$	0.036
$k_W$	Light attenuation constant for water	$m^{-1}$	0.028
$k_C$	Light attenuation constant for chlorophyll	$m^{-1} (mg chl m^{-3})^{-1}$	0.058
$k_D$	Light attenuation constant for detritus	$m^{-1} (mg chl m^{-3})^{-1}$	0.008
$c_{DS0}$	Small detritus decomposition rate at <del>10</del> <u>0</u> $^{\circ}C$	$d^{-1}$	0.001
$c_{DL0}$	Large detritus decomposition rate at <del>10</del> <u>0</u> $^{\circ}C$	$d^{-1}$	0.008
$e_{DON0}$	<del>DON remineraization rate (0-100 m) at 10<math>^{\circ}C</math></del>	<del><math>d^{-1}</math></del>	<del>0.001</del>
	<del>100-500 m at 10<math>^{\circ}C</math></del>	<del><math>d^{-1}</math></del>	<del>0.0002-0.001</del>
	<del>&gt;500 m at 10<math>^{\circ}C</math></del>	<del><math>d^{-1}</math></del>	<del>0.0002</del>
$k_B$	<del>Temp. dependent coefficient for e</del>	<del><math>^{\circ}C^{-1}</math></del>	<del>0.02</del>



**Appendix C: Comparisons in biogeochemical parameters**

<u>Symbol</u>	<u>Parameter</u>	<u>Unit</u>	<u>Yu et al. (2021)</u>	<u>This study</u>
<u>T<sub>0</sub></u>	<u>Limit temperature</u>	<u>°C</u>	<u>10</u>	<u>0</u>
<u>k<sub>B</sub></u>	<u>Temperature dependent coefficient</u>	<u>-</u>	<u>0.002</u>	<u>0.001</u>
<u>C<sub>DON0</sub></u>	<u>DON remineralization constant</u>	<u>d<sup>-1</sup></u>		
	<u>0-100 m</u>		<u>0.001</u>	<u>0.00075</u>
	<u>100-600 m</u>		<u>0.0002-0.001</u>	<u>0.00013-0.00075*</u>
	<u>600-1000 m</u>		<u>0.0002</u>	<u>0.00003-0.00013*</u>

\* C<sub>DON0</sub> decreases with depth by an exponential function.

Code and data availability. The exact version of the software code used to produce the results presented in this paper is archived on Zenodo (<https://doi.org/10.5281/zenodo.5148146>, Wang et al., 2021). Other code and data are available upon request from the authors. Request for materials should be addressed to X.J.W. (xwang@bnu.edu.cn).

Author contributions. X.J.W. and K.W. designed the study, performed the simulations and prepared the manuscript. R.M., D.X.Z. and R.H.Z. contributed to analysis, interpretation of results and writing.

Competing interests. The authors declare that they have no conflict of interest.

Acknowledgements. This work was supported by the Chinese Academy of Sciences' Strategic Priority Project (XDA1101010504). The authors wish to acknowledge the use of the Ferret (<http://ferret.pmel.noaa.gov/Ferret/>).

## References

- Andrews, O., Buitenhuis, E., Le Quere, C., and Suntharalingam, P.: Biogeochemical modelling of dissolved oxygen in a changing ocean, *Philosophical transactions. Series A, Mathematical, physical, and engineering sciences*, 375, 2017.
- 810 Bao, Y. and Li, Y.: Simulations of dissolved oxygen concentration in CMIP5 Earth system models, *Acta Oceanologica Sinica*, 35, 28-37, 2016.
- Beman, J. M., Vargas, S. M., Vazquez, S., Wilson, J. M., Yu, A., Cairo, A., and Perez-Coronel, E.: Biogeochemistry and hydrography shape microbial community assembly and activity in the eastern tropical North Pacific Ocean oxygen minimum zone, *Environmental microbiology*, 23, 2765-2781, 2021.
- 815 Beman, J. M., Vargas, S. M., Vazquez, S., Wilson, J. M., Yu, A., Cairo, A., and Perez-Coronel, E.: Biogeochemistry and hydrography shape microbial community assembly and activity in the eastern tropical North Pacific Ocean oxygen minimum zone, *Environmental microbiology*, 23, 2765-2781, 2020.
- Bertagnolli, A. D. and Stewart, F. J.: Microbial niches in marine oxygen minimum zones, *Nature reviews. Microbiology*, 16, 723-729, 2018.
- 820 Berthet, S., Séférian, R., Bricaud, C., Chevallier, M., Voldoire, A., and Ethé, C.: Evaluation of an Online Grid - Coarsening Algorithm in a Global Eddy - Admitting Ocean Biogeochemical Model, *Journal of Advances in Modeling Earth Systems*, 11, 1759-1783, 2019.
- Bettencourt, J. H., Lopez, C., Hernandez-Garcia, E., Montes, I., Sudre, J., Dewitte, B., Paulmier, A., and Garçon, V.: Boundaries of the Peruvian oxygen minimum zone shaped by coherent mesoscale dynamics, *Nature Geoscience*, 8, 937-U967, 2015.
- 825 Bianchi, D., Dunne, J. P., Sarmiento, J. L., and Galbraith, E. D.: Data-based estimates of suboxia, denitrification, and N<sub>2</sub>O production in the ocean and their sensitivities to dissolved O<sub>2</sub>, *Global Biogeochemical Cycles*, 26, 1-13, 2012.
- Bopp, L., Le Quere, C., Heimann, M., Manning, A. C., and Monfray, P.: Climate-induced oceanic oxygen fluxes: Implications for the contemporary carbon budget, *Global Biogeochemical Cycles*, 16, 1-13, 2002.
- 830 Brandt, P., Bange, H. W., Banyte, D., Dengler, M., Didwischus, S. H., Fischer, T., Greatbatch, R. J., Hahn, J., Kanzow, T., Karstensen, J., Krortzinger, A., Krahnemann, G., Schmidtke, S., Stramma, L., Tanhua, T., and Visbeck, M.: On the role of circulation and mixing in the ventilation of oxygen minimum zones with a focus on the eastern tropical North Atlantic, *Biogeosciences*, 12, 489-512, 2015.
- Breitburg, D., Levin, L. A., Oschlies, A., Gregoire, M., Chavez, F. P., Conley, D. J., Garçon, V., Gilbert, D., Gutierrez, D., 835 Isensee, K., Jacinto, G. S., Limburg, K. E., Montes, I., Naqvi, S. W. A., Pitcher, G. C., Rabalais, N. N., Roman, M. R., Rose, K. A., Seibel, B. A., Telszewski, M., Yasuhara, M., and Zhang, J.: Declining oxygen in the global ocean and coastal waters, *Science*, 359, 2018.
- Busecke, J. J. M., Resplandy, L., and Dunne, J. P. P.: The Equatorial Undercurrent and the Oxygen Minimum Zone in the Pacific, *Geophysical Research Letters*, doi: 10.1029/2019GL082692, 2019. 6716–6725, 2019.
- 840 Cabre, A., Marinov, I., Bernardello, R., and Bianchi, D.: Oxygen minimum zones in the tropical Pacific across CMIP5 models: mean state differences and climate change trends, *Biogeosciences*, 12, 5429-5454, 2015.
- Chen, D., Rothstein, L. M., and Busalacchi, A. J.: A Hybrid Vertical Mixing Scheme and Its Application to Tropical Ocean Models, *Journal of Physical Oceanography*, 24, 2156-2179, 1994.
- Christian, J. R., Verschell, M. A., Murtugudde, R., Busalacchi, A. J., and McClain, C. R.: Biogeochemical modelling of the 845 tropical Pacific Ocean. I: Seasonal and interannual variability, *Deep Sea Research Part II: Topical Studies in Oceanography*, 49, 509-543, 2001.
- Czeschel, R., Stramma, L., and Johnson, G. C.: Oxygen decreases and variability in the eastern equatorial Pacific, *J Geophys Res-Oceans*, 117, 1-12, 2012.
- 850 Czeschel, R., Stramma, L., Schwarzkopf, F. U., Giese, B. S., Funk, A., and Karstensen, J.: Middepth circulation of the eastern tropical South Pacific and its link to the oxygen minimum zone, *J Geophys Res-Oceans*, 116, 2011.
- Duteil, O.: Wind Synoptic Activity Increases Oxygen Levels in the Tropical Pacific Ocean, *Geophysical Research Letters*, 46, 2715-2725, 2019.
- Duteil, O., Frenger, I., and Getzlaff, J.: Intermediate water masses, a major supplier of oxygen for the eastern tropical Pacific ocean, *Ocean Science*, doi: 10.5194/os-2020-17, 2020. 2020.

- 855 Duteil, O. and Oschlies, A.: Sensitivity of simulated extent and future evolution of marine suboxia to mixing intensity, *Geophysical Research Letters*, 38, 2011.
- Feely, R. A., Sabine, C. L., Schlitzer, R., Bullister, J. L., Mecking, S., and Greeley, D.: Oxygen utilization and organic carbon remineralization in the upper water column of the Pacific Ocean, *Journal of Oceanography*, 60, 45-52, 2004.
- 860 Fu, W. W., Bardin, A., and Primeau, F.: Tracing ventilation source of tropical Pacific oxygen minimum zones with an adjoint global ocean transport model, *Deep-Sea Research Part I: Oceanographic Research Papers*, 139, 95-103, 2018.
- Fuenzalida, R., Schneider, W., Garcés-Vargas, J., Bravo, L., and Lange, C.: Vertical and horizontal extension of the oxygen minimum zone in the eastern South Pacific Ocean, *Deep-Sea Res Pt II*, 56, 1027-1038, 2009.
- 865 Garçon, V., Karstensen, J., Palacz, A., Telszewski, M., Aparco Lara, T., Breitburg, D., Chavez, F., Coelho, P., Cornejo-D'Otton, M., Santos, C., Fiedler, B., Gallo, N. D., Grégoire, M., Gutierrez, D., Hernandez-Ayon, M., Isensee, K., Koslow, T., Levin, L., Marsac, F., Maske, H., Mbaye, B. C., Montes, I., Naqvi, W., Pearlman, J., Pinto, E., Pitcher, G., Pizarro, O., Rose, K., Shenoy, D., Van der Plas, A., Vito, M. R., and Weng, K.: Multidisciplinary Observing in the World Ocean's Oxygen Minimum Zone Regions: From Climate to Fish — The VOICE Initiative, *Frontiers in Marine Science*, 6, 2019.
- Gnanadesikan, A., Dunne, J. P., and John, J.: Understanding why the volume of suboxic waters does not increase over centuries of global warming in an Earth System Model, *Biogeosciences*, 9, 1159-1172, 2012.
- 870 Hansell, D. A.: Recalcitrant dissolved organic carbon fractions, *Annual review of marine science*, 5, 421-445, 2013.
- Johnson, K. S., Gordon, R. M., and Coale, K. H.: What controls dissolved iron concentrations in the world ocean?, *Marine Chemistry*, 57, 137-161, 1997.
- Kalnay, E., Kanamitsu, M., Kistler, R., Collins, W., Deaven, D., Gandin, L., Iredell, M., Saha, S., White, G., Woollen, J., Zhu, Y., Chelliah, M., Ebisuzaki, W., Higgins, W., Janowiak, J., Mo, K. C., Ropelewski, C., Wang, J., Leetmaa, A., Reynolds, R., Jenne, R., and Joseph, D.: The NCEP/NCAR 40-year reanalysis project, *B Am Meteorol Soc*, 77, 437-471, 1996.
- 875 Kalvelage, T., Lavik, G., Jensen, M. M., Revsbech, N. P., Loscher, C., Schunck, H., Desai, D. K., Hauss, H., Kiko, R., Holtappels, M., LaRoche, J., Schmitz, R. A., Graco, M. I., and Kuypers, M. M.: Aerobic microbial respiration in oceanic oxygen minimum zones, *PLoS one*, 10, 2015.
- 880 Kalvelage, T., Lavik, G., Lam, P., Contreras, S., Arteaga, L., Löscher, C. R., Oschlies, A., Paulmier, A., Stramma, L., and Kuypers, M. M. M.: Nitrogen cycling driven by organic matter export in the South Pacific oxygen minimum zone, *Nature Geoscience*, 6, 228-234, 2013.
- Karstensen, J., Stramma, L., and Visbeck, M.: Oxygen minimum zones in the eastern tropical Atlantic and Pacific oceans, *Progress in Oceanography*, 77, 331-350, 2008.
- 885 Kuntz, L. B. and Schrag, D. P.: Hemispheric asymmetry in the ventilated thermocline of the Tropical Pacific, *Journal of Climate* 31, 1281-1288, 2018.
- Levin, L. A.: Manifestation, Drivers, and Emergence of Open Ocean Deoxygenation, *Annual review of marine science*, 10, 229-260, 2018.
- 890 Libby, P. S. and Wheeler, P. A.: Particulate and dissolved organic nitrogen in the central and eastern equatorial Pacific, *Deep-Sea Research Part I: Oceanographic Research Papers*, 44, 345-361, 1997.
- Llanillo, P. J., Pelegri, J. L., Talley, L. D., Pena-Izquierdo, J., and Cordero, R. R.: Oxygen Pathways and Budget for the Eastern South Pacific Oxygen Minimum Zone, *Journal of Geophysical Research: Oceans*, 123, 1722-1744, 2018.
- Loginova, A. N., Thomsen, S., Dengler, M., Ludke, J., and Engel, A.: Diapycnal dissolved organic matter supply into the upper Peruvian oxycline, *Biogeosciences*, 16, 2033-2047, 2019.
- 895 Montes, I., Dewitte, B., Gutknecht, E., Paulmier, A., Dadou, I., Oschlies, A., and Garçon, V.: High-resolution modeling of the Eastern Tropical Pacific oxygen minimum zone: Sensitivity to the tropical oceanic circulation, *Journal of Geophysical Research: Oceans*, 119, 5515-5532, 2014.
- Moreno, A. R., Garcia, C. A., Larkin, A. A., Lee, J. A., Wang, W. L., Moore, J. K., Primeau, F. W., and Martiny, A. C.: Latitudinal gradient in the respiration quotient and the implications for ocean oxygen availability, *PNAs*, 117, 22866-22872, 2020.
- 900 Murtugudde, R., Seager, R., and Busalacchi, A.: Simulation of the tropical oceans with an ocean GCM coupled to an atmospheric mixed-layer model, *Journal of Climate*, 9, 1795-1815, 1996.
- Niemeyer, D., Kriest, I., and Oschlies, A.: The effect of marine aggregate parameterisations on nutrients and oxygen minimum zones in a global biogeochemical model, *Biogeosciences*, 16, 3095-3111, 2019.

- 905 Oschlies, A., Brandt, P., Stramma, L., and Schmidtko, S.: Drivers and mechanisms of ocean deoxygenation, *Nature Geoscience*, 11, 467-473, 2018.
- Oschlies, A., Koeve, W., Landolfi, A., and Kahler, P.: Loss of fixed nitrogen causes net oxygen gain in a warmer future ocean, *Nature communications*, 10, 2805, 2019.
- 910 Paulmier, A. and Ruiz-Pino, D.: Oxygen minimum zones (OMZs) in the modern ocean, *Progress in Oceanography*, 80, 113-128, 2009.
- Pavia, F. J., Anderson, R. F., Lam, P. J., Cael, B. B., Vivancos, S. M., Fleisher, M. Q., Lu, Y., Zhang, P., Cheng, H., and Edwards, R. L.: Shallow particulate organic carbon regeneration in the South Pacific Ocean, *Proceedings of the National Academy of Sciences of the United States of America*, 116, 9753-9758, 2019.
- 915 Raimbault, P., Slawyk, G., Boudjellal, B., Coatanoan, C., Conan, P., Coste, B., Garcia, N., Moutin, T., and Pujo-Pay, M.: Carbon and nitrogen uptake and export in the equatorial Pacific at 150°W: Evidence of an efficient regenerated production cycle, *Journal of Geophysical Research: Oceans*, 104, 3341-3356, 1999.
- Schmidtko, S., Stramma, L., and Visbeck, M.: Decline in global oceanic oxygen content during the past five decades, *Nature*, 542, 335-339, 2017.
- Shigemitsu, M., Yamamoto, A., Oka, A., and Yamanaka, Y.: One possible uncertainty in CMIP5 projections of low-oxygen water volume in the Eastern Tropical Pacific, *Geophysical Research Letters*, 31, 804-820, 2017.
- 920 Stramma, L., Johnson, G. C., Firing, E., and Schmidtko, S.: Eastern Pacific oxygen minimum zones: Supply paths and multidecadal changes, *J Geophys Res-Oceans*, 115, 2010.
- Stramma, L., Johnson, G. C., Sprintall, J., and Mohrholz, V.: Expanding oxygen-minimum zones in the tropical oceans, *Science*, 320, 655-658, 2008.
- 925 Stramma, L., Oschlies, A., and Schmidtko, S.: Mismatch between observed and modeled trends in dissolved upper-ocean oxygen over the last 50 yr, *Biogeosciences*, 9, 4045-4057, 2012.
- Sun, X., Frey, C., Garcia-Robledo, E., Jayakumar, A., and Ward, B. B.: Microbial niche differentiation explains nitrite oxidation in marine oxygen minimum zones, *The ISME journal*, 15, 1317-1329, 2021.
- 930 Talley, L. D., Feely, R. A., Sloyan, B. M., Wanninkhof, R., Baringer, M. O., Bullister, J. L., Carlson, C. A., Doney, S. C., Fine, R. A., Firing, E., Gruber, N., Hansell, D. A., Ishii, M., Johnson, G. C., Katsumata, K., Key, R. M., Kramp, M., Langdon, C., Macdonald, A. M., Mathis, J. T., McDonagh, E. L., Mecking, S., Millero, F. J., Mordy, C. W., Nakano, T., Sabine, C. L., Smethie, W. M., Swift, J. H., Tanhua, T., Thurnherr, A. M., Warner, M. J., and Zhang, J. Z.: Changes in ocean heat, carbon content, and ventilation: a review of the first decade of go-ship global repeat hydrography, *Annual review of marine science*, 8, 185-215, 2016.
- 935 Tanioka, T. and Matsumoto, K.: Stability of Marine Organic Matter Respiration Stoichiometry, *Geophysical Research Letters*, 47, 2020.
- Van Mooy, B. A. S., Keil, R. G., and Devol, A. H.: Impact of suboxia on sinking particulate organic carbon: Enhanced carbon flux and preferential degradation of amino acids via denitrification, *Geochimica et Cosmochimica Acta*, 66, 457-465, 2002.
- 940 Wang, W. L., Moore, J. K., Martiny, A. C., and Primeau, F. W.: Convergent estimates of marine nitrogen fixation, *Nature*, 566, 205-211, 2019.
- Wang, X. J., Behrenfeld, M., Le Borgne, R., Murtugudde, R., and Boss, E.: Regulation of phytoplankton carbon to chlorophyll ratio by light, nutrients and temperature in the Equatorial Pacific Ocean: a basin-scale model, *Biogeosciences*, 6, 391-404, 2009a.
- 945 Wang, X. J., Le Borgne, R., Murtugudde, R., Busalacchi, A. J., and Behrenfeld, M.: Spatial and temporal variations in dissolved and particulate organic nitrogen in the equatorial Pacific: biological and physical influences, *Biogeosciences*, 5, 1705-1721, 2008.
- Wang, X. J., Murtugudde, R., Hackert, E., Wang, J., and Beauchamp, J.: Seasonal to decadal variations of sea surface pCO<sub>2</sub> and sea-air CO<sub>2</sub> flux in the equatorial oceans over 1984–2013: A basin-scale comparison of the Pacific and Atlantic Oceans, *Global Biogeochemical Cycles*, 29, 597-609, 2015.
- 950 Wang, X. J., Murtugudde, R., and Le Borgne, R.: Nitrogen uptake and regeneration pathways in the equatorial Pacific: a basin scale modeling study, *Biogeosciences*, 6, 2647-2660, 2009b.
- Wanninkhof, R.: Relationship between wind speed and gas exchange over the Ocean, *J Geophys Res-Oceans*, 97, 7373-7382, 1992.

- 955 Ward, B. A., Wilson, J. D., Death, R. M., Monteiro, F. M., Yool, A., and Ridgwell, A.: EcoGENIE 1.0: plankton ecology in the cGENIE Earth system model, *Geoscientific Model Development*, 11, 4241-4267, 2018.
- Weiss, R. F.: The solubility of nitrogen, oxygen and argon in water and seawater, *Deep-Sea Research*, 17, 721-735, 1970.
- Williams, J. H. T., Totterdell, I. J., Halloran, P. R., and Valdes, P. J.: Numerical simulations of oceanic oxygen cycling in the FAMOUS Earth-System model: FAMOUS-ES, version 1.0, *Geoscientific Model Development*, 7, 1419-1431, 2014.
- 960 Wright, J. J., Konwar, K. M., and Hallam, S. J.: Microbial ecology of expanding oxygen minimum zones, *Nature Reviews Microbiology*, 10, 381-394, 2012.
- Yu, J., Wang, X., Murtugudde, R., Tian, F., and Zhang, R. H.: Interannual - to - Decadal Variations of Particulate Organic Carbon and the Contribution of Phytoplankton in the Tropical Pacific During 1981 - 2016: A Model Study, *Journal of Geophysical Research: Oceans*, 126, 2021.
- 965 Zakem, E. J. and Levine, N. M.: Systematic Variation in Marine Dissolved Organic Matter Stoichiometry and Remineralization Ratios as a Function of Lability, *Global Biogeochemical Cycles*, 33, 1389-1407, 2019.

## Tables

970

**Table 1.** Bias and root mean square error (RMSE) for DO ( $\text{mmol m}^{-3}$ ) comparisons between WOA2013 and model simulations over 1991-2010 in the Eastern Tropical North Pacific (ETNP) and Eastern Tropical South Pacific (ETSP).

<u>Layers</u>	<u>Statistics</u>	<u>Ref</u>	<u>Km6.9</u>	<u>Km18.7</u>	<u>Kb0.25</u>	<u>Kb0.5</u>	<u>Km6.9</u> <u>Kb0.25</u>	<u>Km6.9</u> <u>Kb0.5</u>	<u>Km18.7</u> <u>Kb0.25</u>	<u>Km18.7</u> <u>Kb0.5</u>
<u>ETNP (165°W-90°W, 5°N-20°N)</u>										
<u>200-400 m</u>	<u>Bias</u>	<u>-17.44</u>	<u>-14.84</u>	<u>-11.32</u>	<u>-16.34</u>	<u>-14.87</u>	<u>-13.51</u>	<u>-11.85</u>	<u>-9.71</u>	<u>-7.8</u>
	<u>RMSE</u>	<u>16.35</u>	<u>14.63</u>	<u>12.43</u>	<u>15.73</u>	<u>14.91</u>	<u>13.83</u>	<u>12.84</u>	<u>11.4</u>	<u>10.2</u>
<u>400-700 m</u>	<u>Bias</u>	<u>-16.35</u>	<u>-14.95</u>	<u>-12.51</u>	<u>-11.85</u>	<u>-7.5</u>	<u>-9.98</u>	<u>-5.39</u>	<u>-6.88</u>	<u>-2.04</u>
	<u>RMSE</u>	<u>10.6</u>	<u>9.83</u>	<u>8.45</u>	<u>8.26</u>	<u>6.73</u>	<u>7.49</u>	<u>6.38</u>	<u>6.5</u>	<u>6.78</u>
<u>700-1000 m</u>	<u>Bias</u>	<u>-9.22</u>	<u>-8.32</u>	<u>-5.99</u>	<u>-3.58</u>	<u>0.62</u>	<u>-2.71</u>	<u>1.38</u>	<u>-5.75</u>	<u>3.27</u>
	<u>RMSE</u>	<u>5.1</u>	<u>4.29</u>	<u>2.64</u>	<u>2.93</u>	<u>6.52</u>	<u>3.59</u>	<u>7.19</u>	<u>5.39</u>	<u>9.08</u>
<u>ETSP (110°W-80°W, 10°S-3°S)</u>										
<u>200-400 m</u>	<u>Bias</u>	<u>-7.09</u>	<u>-3.91</u>	<u>0.19</u>	<u>-6.43</u>	<u>-5.39</u>	<u>-2.84</u>	<u>-1.13</u>	<u>2.09</u>	<u>4.85</u>
	<u>RMSE</u>	<u>7.39</u>	<u>4.46</u>	<u>2.36</u>	<u>6.83</u>	<u>5.98</u>	<u>3.69</u>	<u>2.86</u>	<u>3.27</u>	<u>5.51</u>
<u>400-700 m</u>	<u>Bias</u>	<u>-11.3</u>	<u>-10.43</u>	<u>-7.94</u>	<u>-5.94</u>	<u>-0.88</u>	<u>-4.51</u>	<u>1.34</u>	<u>-1.21</u>	<u>5.23</u>
	<u>RMSE</u>	<u>12.98</u>	<u>12.15</u>	<u>10.06</u>	<u>8.52</u>	<u>6.03</u>	<u>7.41</u>	<u>5.65</u>	<u>5.81</u>	<u>7.38</u>
<u>700-1000 m</u>	<u>Bias</u>	<u>-7.3</u>	<u>-7.08</u>	<u>-5.13</u>	<u>-0.97</u>	<u>3.38</u>	<u>-0.62</u>	<u>3.94</u>	<u>1.05</u>	<u>5.46</u>
	<u>RMSE</u>	<u>12.82</u>	<u>12.49</u>	<u>11.22</u>	<u>8.98</u>	<u>8.63</u>	<u>8.76</u>	<u>8.68</u>	<u>8.59</u>	<u>9.34</u>

975

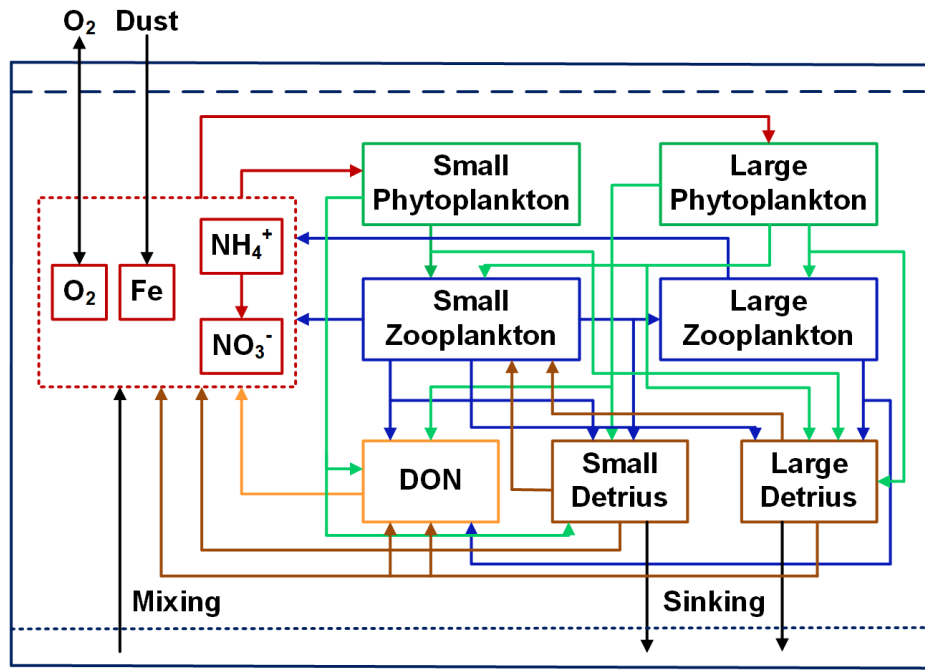
**Table 2.** Volumes ( $10^{15} \text{ m}^3$ ) of suboxic and hypoxic water from WOA2013 and model simulations.

<u>Regions</u>	<u>Waters</u>	<u>WOA2013</u>	<u>Reference</u>	<u>Km6.9</u>	<u>Km18.7</u>	<u>Kb0.25</u>	<u>Kb0.5</u>	<u>Km6.9</u> <u>Kb0.25</u>	<u>Km6.9</u> <u>Kb0.5</u>	<u>Km18.7</u> <u>Kb0.25</u>	<u>Km18.7</u> <u>Kb0.5</u>
<u>North</u> <u>Pacific</u>	<u>Suboxic</u>	<u>5.97</u>	<u>10.61</u>	<u>9.98</u>	<u>8.83</u>	<u>8.73</u>	<u>7.33</u>	<u>8.08</u>	<u>6.68</u>	<u>6.88</u>	<u>5.55</u>
	<u>Hypoxic</u>	<u>19.98</u>	<u>22.67</u>	<u>22.5</u>	<u>22.17</u>	<u>22.32</u>	<u>21.61</u>	<u>22.11</u>	<u>21.35</u>	<u>21.71</u>	<u>20.91</u>
<u>South</u> <u>Pacific</u>	<u>Suboxic</u>	<u>1.43</u>	<u>3.78</u>	<u>3.39</u>	<u>2.78</u>	<u>2.86</u>	<u>2.15</u>	<u>2.42</u>	<u>1.71</u>	<u>1.81</u>	<u>1.12</u>
	<u>Hypoxic</u>	<u>7.12</u>	<u>10.42</u>	<u>10.21</u>	<u>9.8</u>	<u>9.19</u>	<u>8.17</u>	<u>8.94</u>	<u>7.88</u>	<u>8.49</u>	<u>7.39</u>

Suboxic: DO <20  $\text{mmol m}^{-3}$ ; Hypoxic: DO <60  $\text{mmol m}^{-3}$ .



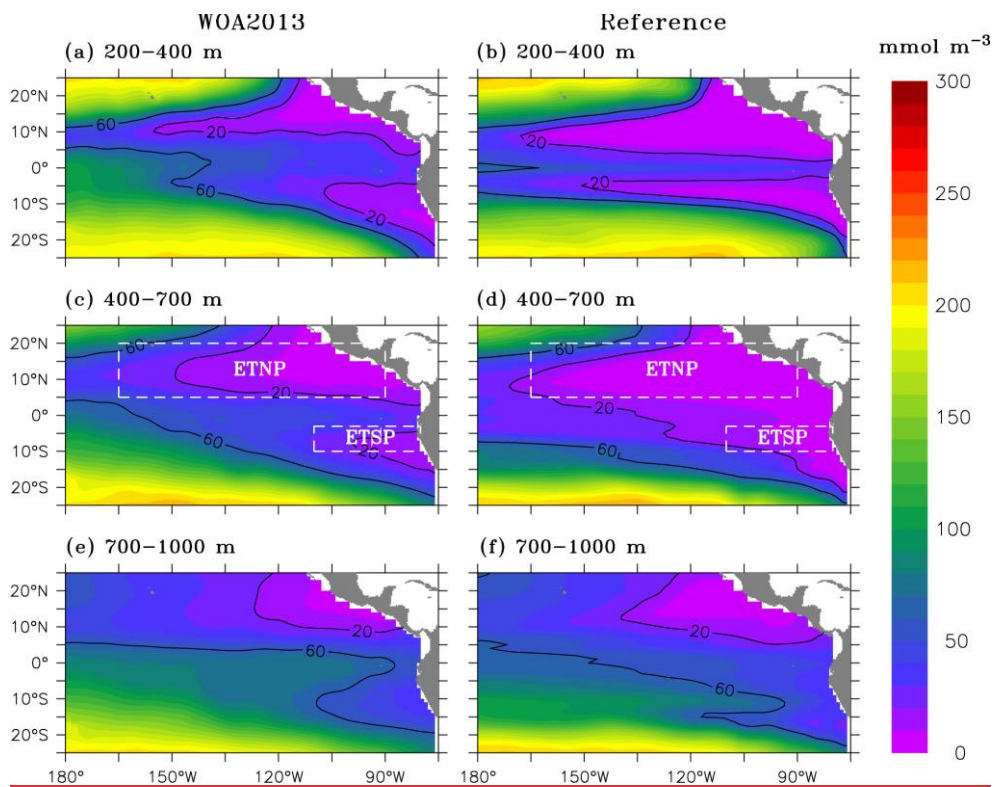
Figures



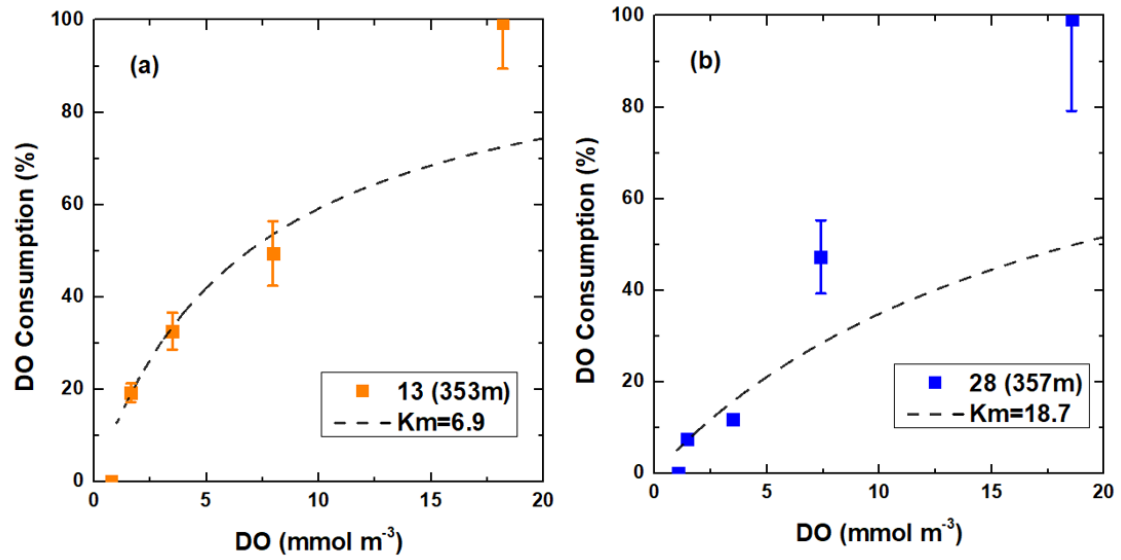
980

Figure 1. Flow diagram of ecosystem model. Red, green, blue, yellow and brown lines and arrows denote fluxes originating from inorganic forms, phytoplankton, zooplankton, DON and detritus, respectively.

985



990 **Figure 2.** Comparisons of DO concentration between WOA2013 (left panel) and reference run (right panel) during 1991-2010. White dash lines in (c) and (d) denotes two boxes for ETNP (165°W-90°W, 5°N-20°N) and ETSP (110°W-80°W, 10°S-3°S).



**Figure 3.** Biological consumption vs. DO concentration at (a) station 13 (353 m) and (b) station 28 (357 m) in the Peruvian OMZ. Data are from Kalvelage (2015).

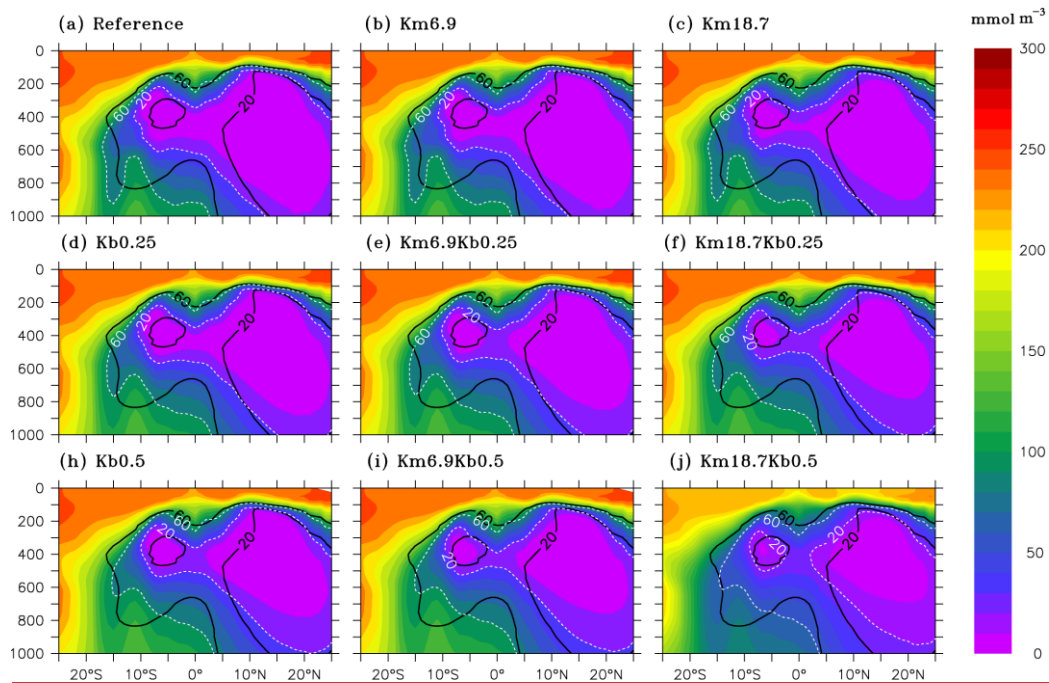


**Figure 4.** Vertical distribution of DO and asymmetric OMZs over 120°W-90°W from different model simulations for (a) reference run, (b and c) reduced O:C utilization ratio, (d and h) enhanced vertical mixing, and (e, f, i, and j) combination of reduced O:C utilization ratio and enhanced vertical mixing. Black lines denote contours of DO concentrations of 20 mmol m<sup>-3</sup> and 60 mmol m<sup>-3</sup> from WOA2013 data.

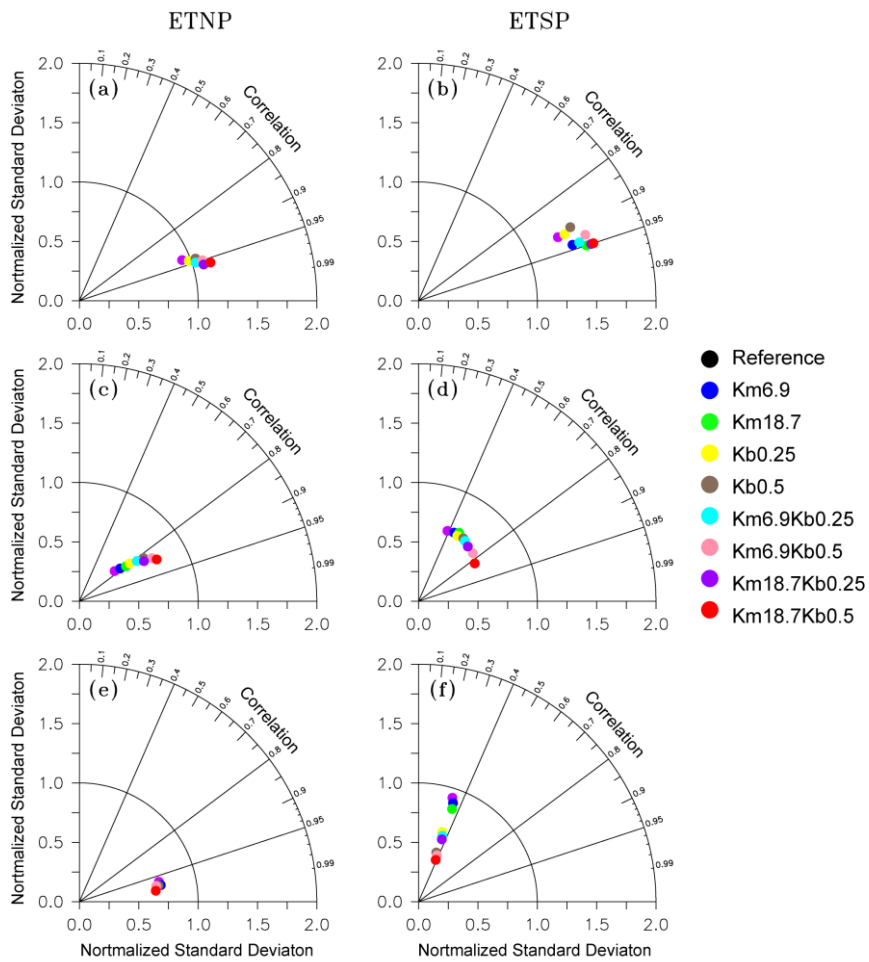
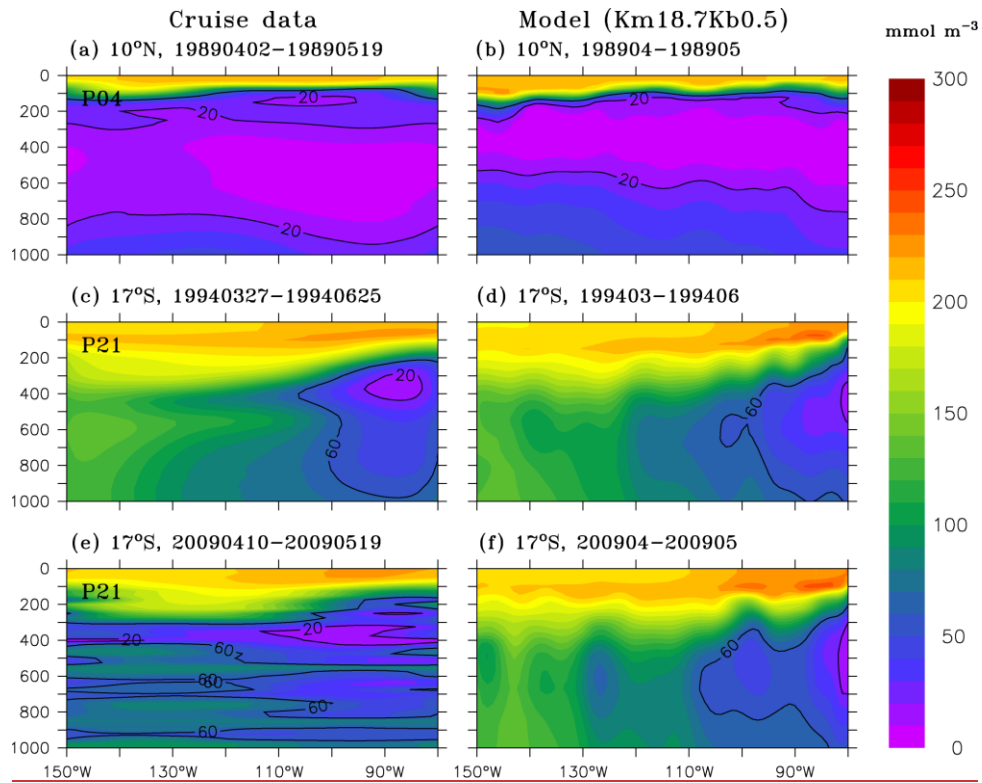


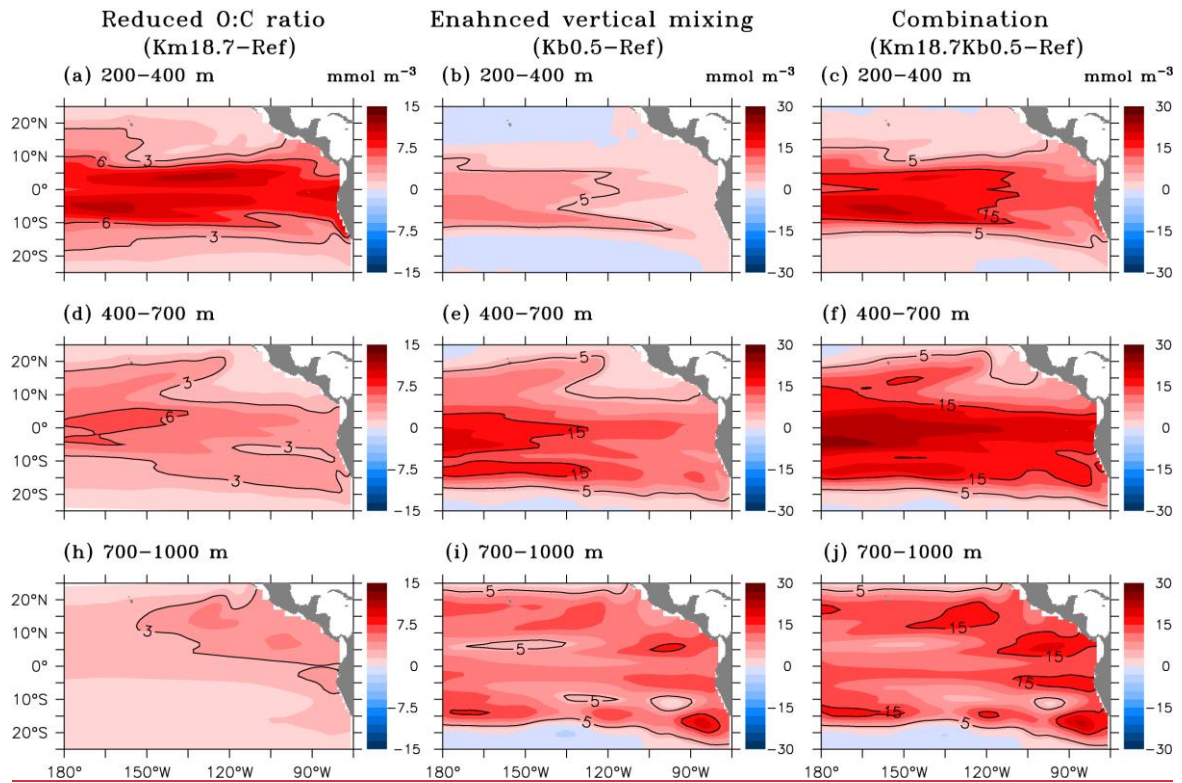
**Figure 5.** Taylor diagrams for the performance of simulated DO concentration (against WOA2013) from model simulations for ETNP (165°W-90°W, 5°N-20°N, left panel) and ETSP (110°W-80°W, 10°S-3°S, right panel) over (a and b) 200-400 m, (c and d) 400-700 m, and (e and f) 700-1000 m.

1010



1015

**Figure 6.** Distribution of DO from cruise data (left panel) and model simulation from the Km18.7Kb0.5 (see text for explanation; right panel). Observed DO along the P04 and P21 lines are from CCHDO (<https://cchdo.ucsd.edu/>).



1020

**Figure 7.** Changes of DO concentration averaged over (a, b and c) 200-400 m, (d, e and f) 400-700 m, and (h, i and j) 700-1000 m due to reduced O:C utilization ratio (left panel), enhanced vertical mixing (middle panel), and the combination of reduced O:C utilization ratio and enhanced vertical mixing (right panel).

1025



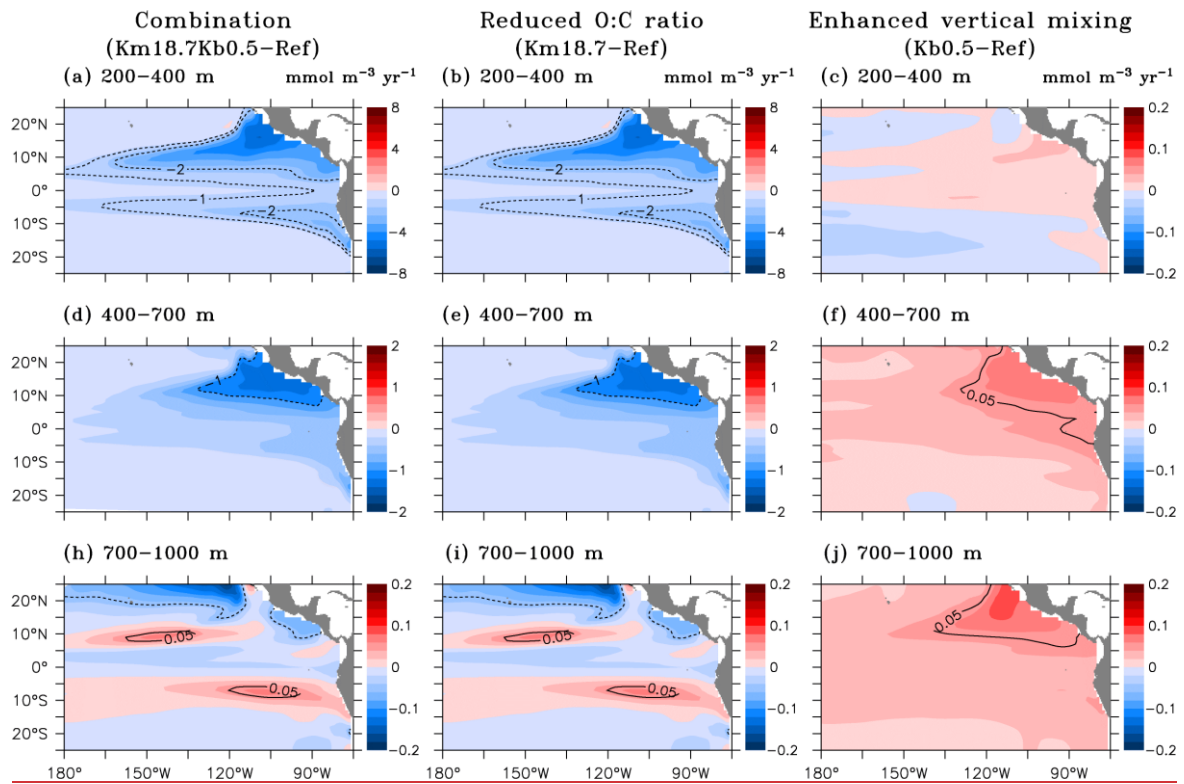
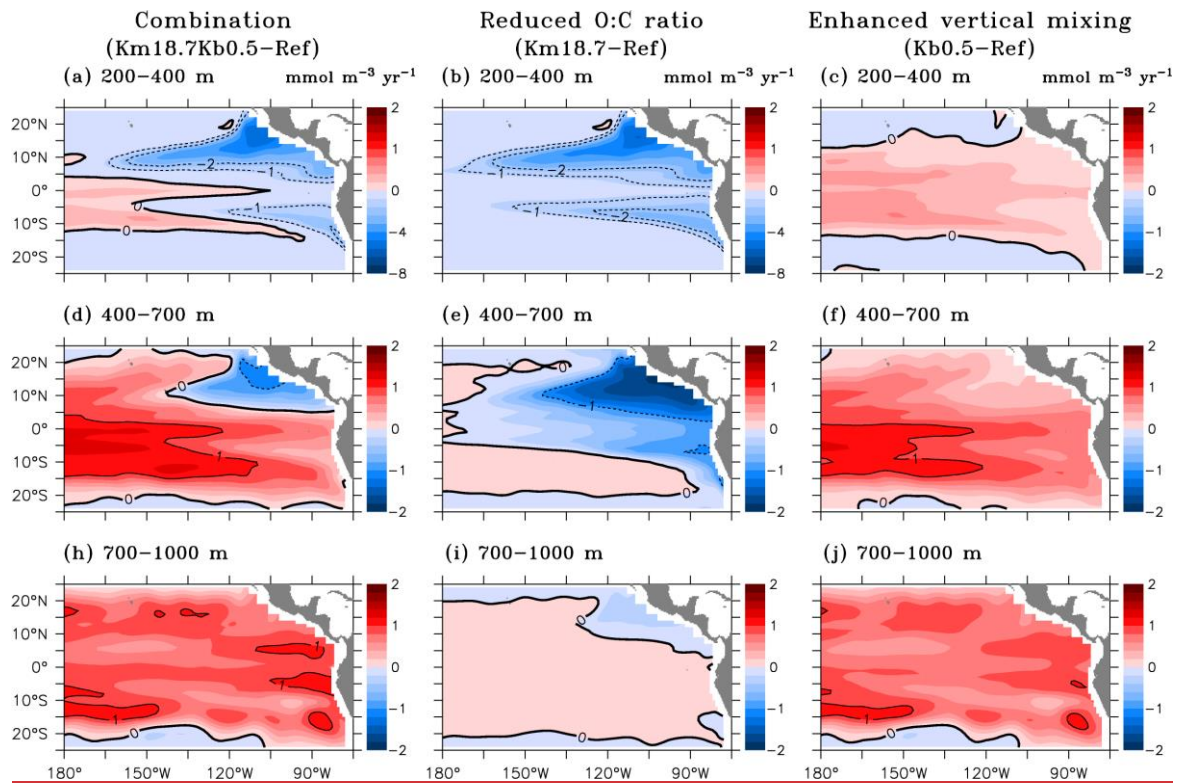


**Figure 8.** Changes in biological consumption over (a, b and c) 200-400 m, (d, e and f) 400-700 m, and (h, i and j) 700-1000 m due to the combination of reduced O:C utilization ratio and enhanced vertical mixing (left panel), reduced O:C utilization ratio (middle panel), and enhanced vertical mixing (right panel).

1030



1035

**Figure 9.** Changes in physical supply due to over (a, b and c) 200-400 m, (d, e and f) 400-700 m, and (h, i and j) 700-1000 m the combination of reduced O:C utilization ratio and enhanced vertical mixing (left panel), reduced O:C utilization ratio (middle panel), and enhanced vertical mixing (right panel).

1040

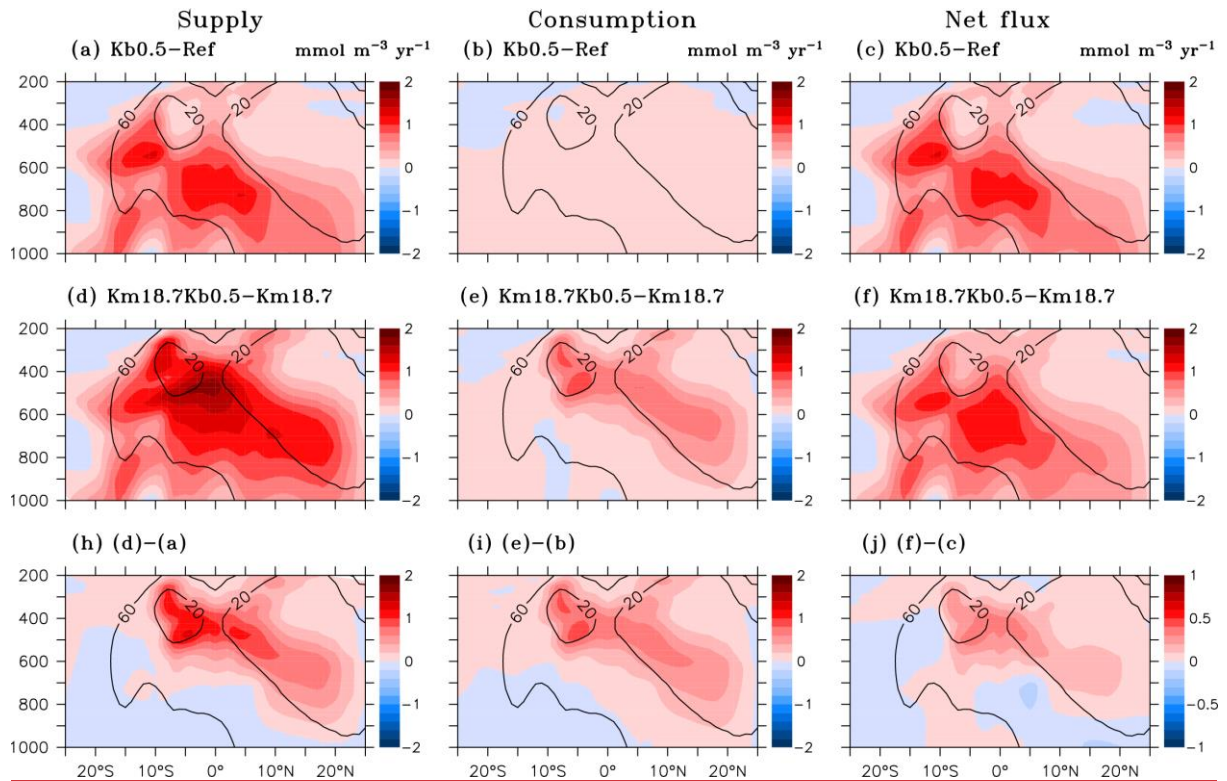
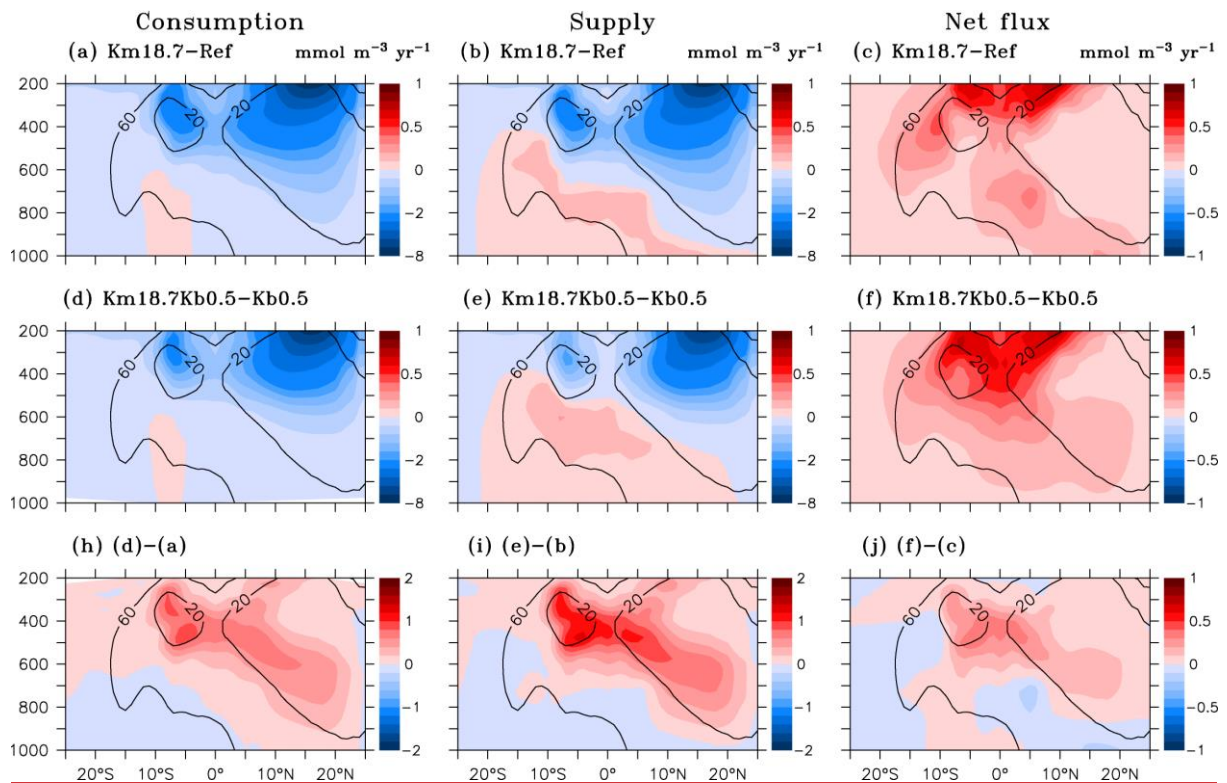
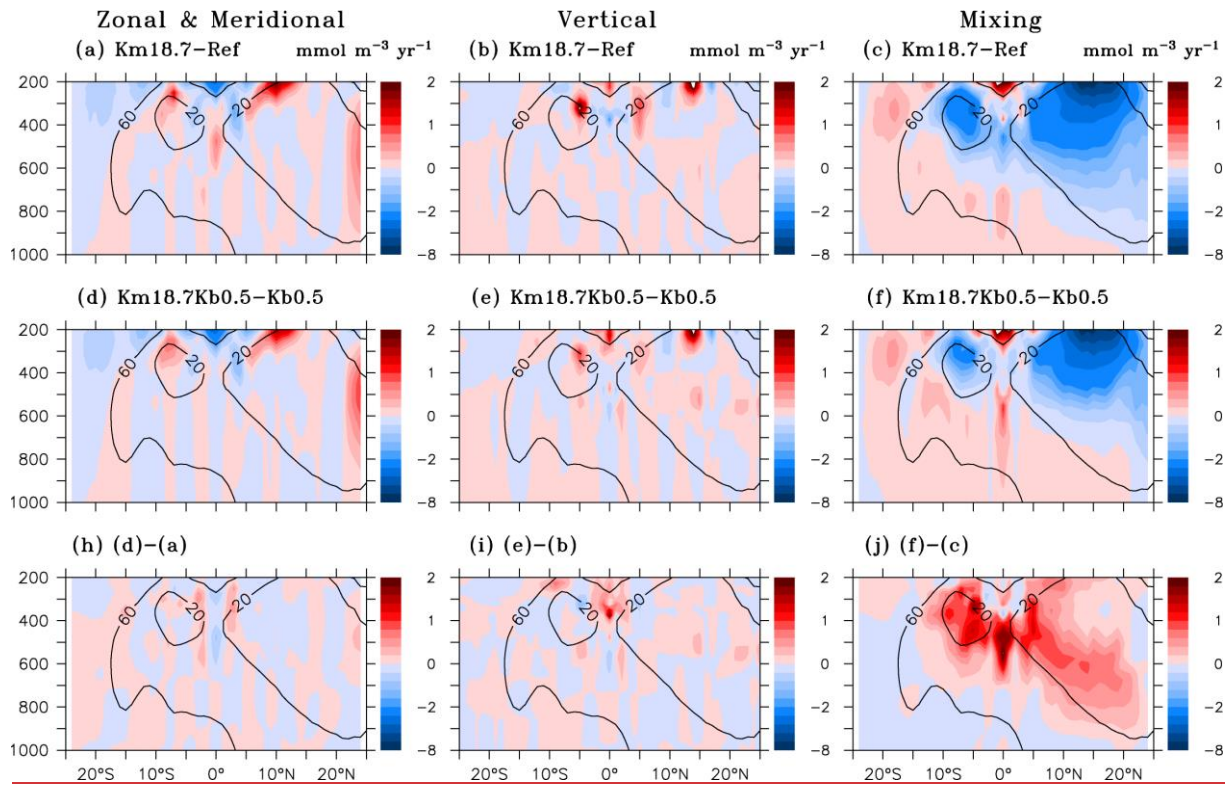


**Figure 10.** Changes in physical supply (left panel), biological consumption (middle panel), and net flux (right panel) under enhanced vertical mixing with (d, e, and f, middle row) and without (a, b, and c, top row) reduced O:C utilization ratio, and the differences between them (h, i, and j, bottom row).

1045



1050 **Figure 11.** Changes in biological consumption (left panel), physical supply (middle panel), and net flux (right panel) under a reduced O:C utilization ratio with (d, e, and f, middle row) and without enhanced vertical mixing (a, b, and c, top row), and the differences between them (h, i, and j, bottom row).



1055

**Figure 12.** Changes and differences in zonal and meridional advections (left panel), vertical advection (middle pane), and vertical mixing (right panel) under a reduced O:C utilization ratio with (d, e, and f, middle row) and without enhanced vertical mixing (a, b, and c, top row), and the differences between them (h, i, and j, bottom row).